Chapter 1

A Continuum Theory of Flexoelectricity

Qian Deng*
Department of Mechanical Engineering, University of Houston, Houston, TX 77024, USA

Liping Liu†
Department of Mathematics and Department of Mechanical Aerospace Engineering, Rutgers University, Piscataway, NJ 08854, USA

Pradeep Sharma‡
Department of Mechanical Engineering, University of Houston, Houston, TX 77024, USA

In this chapter we present a nonlinear continuum theory of flexoelectricity. Due to the scaling of strain gradients with structural feature size, flexoelectricity is expected to show a strong size dependency in electromechanical coupling. Aside from several illustrative and pedagogical boundary value problems, we present examples that highlight the applications of flexoelectricity e.g. creation of piezoelectric materials without using piezoelectric materials, energy harvesting, soft active materials and biological membranes.

1. Introduction

Recently, a somewhat understudied electromechanical coupling, flexoelectricity, has attracted a fair amount of attention from both fundamental and applications points of view leading to intensive experimental[1–9] and theoretical[10–22] activity in this topic. To understand flexoelectricity better, it

*qdeng@central.uh.edu.
†liu.liping@rutgers.edu
‡psharma@uh.edu.

is best first to allude to the central mathematical relation that describes piezoelectricity:

$$P_i \sim d_{ijk}\varepsilon_{jk} \tag{1}$$

In equation (1), the polarization vector P_i is related to the second order strain tensor ε_{jk} through the third order piezoelectric material property tensor d_{ijk}. Tensor transformation properties require that under inversion-center symmetry, all odd-order tensors vanish. Thus, most common crystalline materials, e.g. Silicon, and NaCl are not piezoelectric whereas ZnO and GaAs are. Physically, however, it is possible to visualize how a non-uniform strain or the presence of strain gradients may potentially break the inversion symmetry and induce polarization even in centrosymmetric crystals.[23–27] This is tantamount to extending relation (1) to include strain gradients:

$$P_i \sim d_{ijk}\varepsilon_{jk} + f_{ijkl}\frac{d\varepsilon_{jk}}{dx_l} \tag{2}$$

where f_{ijkl} are the components of the so-called flexoelectric tensor. While the piezoelectric property is non-zero only for selected materials, the strain gradient-polarization coupling (i.e. flexoelectricity tensor) is in principle non-zero for all (insulating) materials. This implies that under a non-uniform strain, all dielectric materials are capable of producing a polarization.[28] The flexoelectric mechanism is well-illustrated by the non-uniform straining of a graphene nanoribbon—a manifestly non-piezoelectric material (Fig.1(a)).[22,29] As another widely studied two dimensional soft materials, biological membranes also show flexoelectricity (Fig.1(b)).[30–32] Flexoelectricity has been experimentally confirmed in several crystalline materials such as NaCl, ferroelectrics like Barium Titanate among others.[8,9] Recent works, some of which are summarized elsewhere in this book, have provided important insights into the atomistic origins of flexoelectricity in crystalline solids.[12,33–39] The mechanisms of flexoelectricity in polymers (while experimentally proven) still remain unclear[40–42] and atomistic modeling (being conducted by the authors) is expected to shed light on this issue in the near future. We speculate that the presence of frozen dipoles and their thermal fluctuations is the cause of flexoelectricity in soft materials, however, we cannot offer a more definitive explanation at this point and simply emphasize that this phenomenon has been experimentally confirmed[40–42] and further elucidation is a subject of future research.

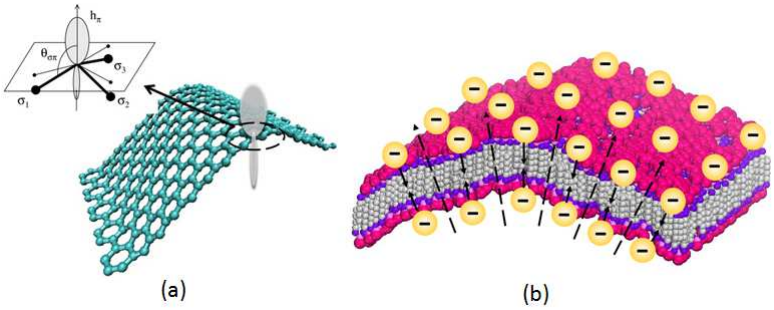

Fig. 1. Flexoelectricity in membranes. (a) Bending of graphene: upon bending, the symmetry of the electron distribution at each atomic site is broken, which leads to the polarization normal to the graphene ribbon; An infinite graphene sheet is semi-metallic however finite graphene nanoribbons can be dielectric depending upon surface termination. (b) Bending of a lipid bilayer membrane: Due to bending, both the charge and dipole densities in the upper and lower layers become asymmetric. This asymmetry causes the normal polarization in the bilayer membrane. Reprinted with permission from ELSEVIER.[43] Copyright 2014.

Flexoelectricity results in the size-dependency of electromechanical coupling and researchers (including us) have advocated several tantalizing applications that can result through its exploitation. For example, the notion of creating piezoelectric materials without using piezoelectric materials,[9,17,18,29] giant piezoelectricity in inhomogeneously deformed nanostructures,[13,15] enhanced energy harvesting,[14,16] the origins of nanoindentation size effects,[20] renormalized ferroelectric properties,[6,10,11,44] the origins of the dead-layer effect in nano capacitors[45] among others. In fact, Chandratre and Sharma[29] have recently shown that graphene can be coaxed to behave like a piezoelectric material merely by creating holes of certain symmetry. The artificial piezoelectricity thus produced was found to be almost as strong as that of well-known piezoelectric substances such as quartz. Such a constructed graphene nano ribbon may be considered to be the thinnest known piezoelectric material. We briefly elaborate on this notion (Fig. 2). Consider a material consisting of two or more different non-piezoelectric dielectrics—as a concrete example that has been studied in the past we may think of a (dielectric) graphene nano ribbon impregnated with holes (Fig.2(a)).[29] Upon the application of uniform stress, differences in material properties at the interfaces of the materials will result in the presence of strain gradients. Those gradients will induce polarization due to the flexoelectric effect. As long as certain symmetry rules are

followed, the net average polarization will be nonzero. Thus, the artificially structured material will exhibit an electrical response under uniform stress behaving therefore like a piezoelectric material. The length scales must be "small"since this concept requires very large strain gradients and those for a given strain are generated easily only at the nanoscale. Here we mention that the precise scale at which this effect becomes prominent depends on the strength of the flexoelectric coefficients. For several materials studied, sub-10 nm characteristic length scales are required albeit (as this study will also show) this effect can also manifest with feature size of less than a micron. Regarding symmetry: Topologies of only certain symmetries can realize the aforementioned concept. For example, circular holes distributed in a material will not yield apparently piezoelectric behavior even though the flexoelectric effect will cause local polarization fields. Due to circular symmetry, the overall average polarization is zero. A similar material but containing triangular shaped holes (or inclusions) for example, and aligned in the same direction, will exhibit the required apparent piezoelectricity. In a similar vein, a finite bilayer or multilayer configuration may also be used (Fig.2(b))–see discussions in.[18]

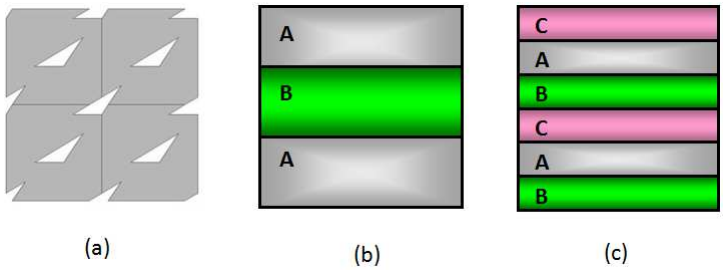

Fig. 2. Creating a piezoelectric material without using piezoelectric materials. (a) A material with a second phase, under a uniform stress, will produce local strain gradients and hence local polarization due to flexoelectricity. If the shape of the second phase is non-centrosymmetrical, the average polarization will be non-zero as well thus, from a macroscopic viewpoint, exhibiting a piezoelectric like effect. In this figure, this concept is illustrated by riddling a sheet with triangular holes. Such a sheet, with circular holes will yield a net zero average polarization. (b) The concept may also be realized by using a superlattice of differing materials. However, here care must be taken. A bilayer superlattice will result in a zero average polarization and (c) a trilayer superlattice is required to break the requisite symmetry. Nevertheless, finite bilayers (due to symmetry breaking at the free surfaces) will produce this effect. Reprinted with permission from ELSEVIER.[43] Copyright 2014.

In this chapter we present a nonlinear continuum framework for flexoelectricity. It is worthwhile to mention that in finite dielectrics, because of the breaking of symmetry at the surfaces and interfaces, the so-called *surface* flexoelectric and piezoelectric effects may also play an important role.[24,46–48] However, in our current framework, we have just considered bulk flexoelectricity and ignored surface effects. In addition to the discussions by Tagantsev and others,[24,46–48] a recent work by one of us has also highlighted some aspects of this surface behavior.[49] Through the solution to various illustrative boundary value problems, we highlight the notable features and the applications of the presented framework. In Section 2, the governing equations and the associated boundary conditions are derived. In Section 3, we illustrate the notion of creating piezoelectric materials without using piezoelectric materials by solving the boundary value problem of a thin film layered superlattice structure. In Section 4, we present the solution of a truncated cone under uniaxial compression. This solution is useful in the experimental extraction of flexoelectric properties. In Section 5, we consider the bending and dynamical vibration of a beam and implications for energy harvesting are explored. In Section 6, we analyze the flexoelectric response of a biological membrane and finally, in Section 7, we consider nonlinear effects in the context of flexoelectricity in soft materials.

2. Continuum Theory of Flexoelectricity

2.1. *Continuum kinematics*

Consider a deformable continuum body as shown in Fig. 3. Let the three-dimensional region occupied by the undeformed body be denoted Ω_R, with the boundary $\partial\Omega_R$. The position of a material point $\mathbf{A}$ in Ω_R can be described by the coordinate system X_K $(K = 1, 2, 3)$. After deformation $\boldsymbol{\chi}$, the material point $\mathbf{A}(X_K)$ moves to the new position $\mathbf{a}(x_k)$, where x_k $(k = 1, 2, 3)$ denotes a new coordinate system associated with the deformed body that occupies the region Ω. These two coordinate systems need not be identical. In traditional continuum mechanics, we call X_K the material or Lagrangian coordinates and x_k the spatial or Eulerian coordinates. Three base vectors for material coordinate system and the spatial coordinate system are respectively denoted by $\mathbf{I}_K$ and $\mathbf{i}_k$.The deformation $\boldsymbol{\chi}$ may be understood as a mapping from the material coordinates to the spatial coordinates, $\boldsymbol{\chi} = \mathbf{x}(\mathbf{X})$. We will also refer to the undeformed body as the reference configuration and the deformed body as the current configura-

tion. In this chapter, all the quantities in the reference configuration are denoted by capital letters and the lower-case letters are used to describe those quantities in the current configuration.

Based on the above setup, the deformation gradient $F_{kK} \equiv x_{k,K} = \partial x_k/\partial X_K$ is introduced here. In the rest of this chapter, for the convenience of presentation, we use "$,K$" and "$,k$" to represent the partial derivatives with respect to the coordinates X_K and x_k, respectively. Unless specified otherwise, the Einstein summation convention is applied throughout the chapter. The determinant of the deformation gradient is the so-called Jacobian which is denoted by $J \equiv det(x_{k,K})$. This scalar field describes the change of a infinitesimal volume dV after deformation through the relationship $dv = JdV$. Thus the mass density field $\rho_0(X_K)$ of the undeformed body is related to its counterpart $\rho(x_k(X_K))$ in the deformed body by $\rho_0(X_K) = J\rho(X_K)$ due to the assumption of local mass conservation. A similar relationship also holds between the charge density field $\rho_0^e(X_K)$ and $\rho^e(x_k(X_K))$, $\rho_0^e(X_K) = J\rho^e(X_K)$.

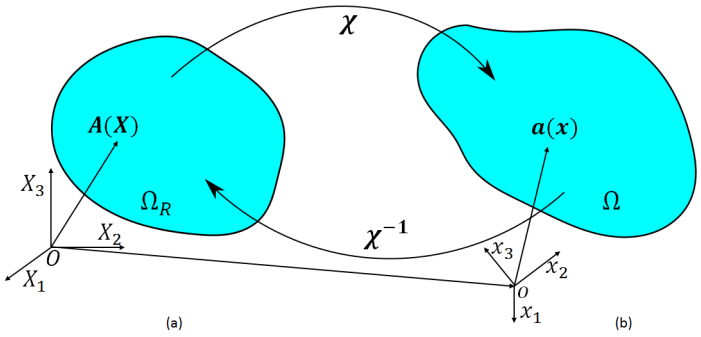

Fig. 3. (a) Reference and (b) current configurations.

2.2. *Maxwell's equations*

To account for energies associated with electric fields and loading devices, we shall first solve for the electric field via the Maxwell equations, i.e., the electric field $e_k = -\phi_{,k}$ in the current configuration is determined by

$$d_{k,k} = \epsilon_0 e_{k,k} + p_{k,k} + p^e_{k,k} = \rho^e \tag{3}$$

where ϕ is the electrostatic potential, $d_k = \epsilon_0 e_k + p_k + p^e_k$ is the electric displacement field, ϵ_0 is the permittivity of free space, p_k is the intrinsic

polarization, p_k^e is the external polarization and ρ^e is the external charge density. By *external* we refer to polarization or charge density that does not change during the deformation or electrical stimulus process. In standard electrostatics textbooks, in the context of charge, this would be identical to the so-called free-charge.

Before proceeding further, it is worthwhile to examine our use of the notion of a *polarization density field*. While this is fairly standard in classical continuum mechanics (as evident in most field theory papers cited in this chapter), recent developments in the physics literature, in the context of periodic solids, have brought to light the fact that the polarization density field depends on the choice of the unit cell. The reader is referred to the paper by Resta and Vanderbilt[50] and references therein for a detailed discussion on this matter and how the concept of the so-called Berry phase has been used to resolve this controversy. Notwithstanding this and other related works, we wish to point out a very important observation made by Marshall and Dayal:[51] If we start with a *finite* periodic solid and then examine its limit (to an infinite size) *correctly* accounting for surface and bulk bound charges, the physically relevant quantities (such as the energies and forces) are *uniquely* determined—independent of the choice of the unit cell used to compute the polarization field density. A different choice of the unit cell will lead to a different polarization density field. However, corresponding to this change in the bulk bound charges, the surface charges will change accordingly to yield exactly the same electric field and energy. Marshall and Dayal[51] draw an analogy analogy of this situation to the definition of the strain field. Calculation of the strain field depends on the choice of the reference configuration. Nevertheless, as long as the calculations are then carried out consistently, the physically relevant quantities, such as the change in the elastic energy, are uniquely determined.

It is known that the electric field e_k, polarization p_k, and even charge density ρ^e can experience a change due to the deformation of the dielectric material. This renders the variational calculations of the field equations a bit tedious. To facilitate such calculations, it is beneficial to pull back all field quantities to the reference configuration (prior to deformation). Particularly in the case of polarization and other electrical quantities, this is a mathematical artifact but a useful one—-and a standard one in continuum mechanics of electromechanical deformable media. The quantities after the

pull-back are given by:

$$\begin{aligned} &E_K = e_k x_{k,K}, \quad P_K = J p_k \alpha_{kK}, \\ &D_K = J X_{K,k} d_k, \quad P^e_K = J p^e_k \alpha_{kK}, \\ &\rho^e_0 = J \rho^e \end{aligned} \tag{4}$$

where $\alpha_{kK} = \mathbf{i}_k \cdot \mathbf{I}_K$ is called the shifter which may be viewed as the rotation from the coordinate frame $\mathbf{I}_K$ to $\mathbf{i}_k$.

Upon a change of variables, in the reference configuration, we can rewrite the Maxwell equations (3) as

$$D_{K,K} = (\epsilon_0 J X_{K,k} X_{L,k} E_L + X_{K,k} \alpha_{kL} P_L + X_{K,k} \alpha_{kL} P^e_L)_{,K} = \rho^e_0 \tag{5}$$

where $D_K = J X_{K,k} d_k = \epsilon_0 J X_{K,k} X_{L,k} E_L + X_{K,k} \alpha_{kL} (P_L + P^e_L)$ is the nominal electric displacement which corresponds to the electric displacement if there is only electric field but no deformation applied to the dielectric body. The identity[52] $(J X_{K,k})_{,K} = 0$ is used to obtain the last equality of (5).

2.3. *Free energy of an electromechanical system*

To model flexoelectricity, we postulate that the internal/stored energy of the system is given by

$$U[x_k, P_K] = \int_{\Omega_R} \psi(F_{kK}, G_{kKL}, P_K, \Pi_{KL}) \tag{6}$$

where $G_{kKL} = x_{k,KL}$ and $\Pi_{KL} = P_{K,L}$ correspond to the gradient of deformation gradient F_{kK} and the nominal polarization P_K, respectively. Note that if we remove the dependency of the internal energy on the terms G_{kKL} and Π_{KL}, our formulation will reduce to classical elasticity of soft dielectric materials.[52,53] As will be shown later in this section, the dependence of the internal energy on $G_{kKL} = x_{k,KL}$ and $\Pi_{KL} = P_{K,L}$, leads to high order flux terms that enter both the Euler-Lagrange equations and the boundary conditions.

The boundary conditions also contribute to the free energy of the deformable dielectric system. Fig.4 depicts the schematic of the problem where the (generally possible) electrical and mechanical boundary conditions are indicated. For this system, we identify the total free energy of the system as[54]

$$F[x_k, P_K] = U[x_k, P_K] + \varepsilon^{elect}[x_k, P_K] + P^{mech}[x_k] \tag{7}$$

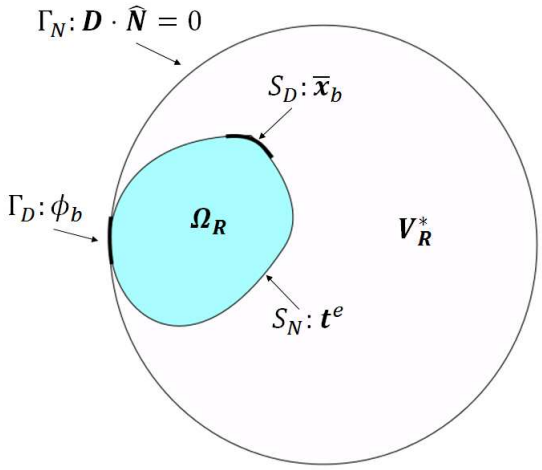

Fig. 4. A deformable dielectric system with electrical and mechanical boundary conditions ($\hat{\mathbf{N}}$ denotes the normal vector of ∂V_R^*).

where

$$\varepsilon^{elect}[x_k, P_K] = \frac{\epsilon_0}{2}\int_{\Omega+V*} e_k e_k dv + \int_{\Gamma_D} \phi_b N_K D_K dA \tag{8}$$

is the total electric energy associated with the electric field and the boundary electric device, V^* is the space outside the body Ω, Γ_D is the Dirichlet boundary where the potential is set to ϕ_b, n_k is the normal vector of Γ_D, and

$$P^{mech}[x_k] = -\int_{S_N} t_K^e x_k \alpha_{Kk} dA - \int_{\Omega_R} B_K^e x_k \alpha_{Kk} dV \tag{9}$$

is the potential energy of mechanical loading with t_K^e being the surface traction applied on S_N and B_K^e being the applied body force.

It is also worthwhile to mention that, for given polarization p_k, we can solve the Maxwell equation (3) with boundary conditions for a unique electric field e_k, and hence the electric energy (8) is well defined.

2.4. *Governing equations*

By the principle of minimum free energy, the equilibrium state of the system is determined by

$$\min_{(x_k, P_K)\in\mathcal{S}} F[x_k, P_K] \tag{10}$$

with the constraint of Maxwell equation (3) or (5), where S is a suitable space for the state variables such that sufficient smoothness and boundedness is ensured.

To find the Euler-Lagrange equations associated with a minimizer (10), we consider variations of

(1) polarization

$$x_k \to x_k, \qquad P_K \to P_K + \delta Q_K \tag{11}$$

(2) deformation

$$x_k \to x_k + \delta u_k, \qquad P_K \to P_K \tag{12}$$

where δ is a small number which controls the magnitude of the variations, Q_K and u_k are admissible variations of the field variables P_K and x_k, respectively.

We first consider the variation of polarization (11). Standard variational calculations yield:

$$\begin{aligned}
&\frac{d}{d\delta}F[x_k, P_K + \delta Q_K]|_{\delta=0} \\
&= \frac{d}{d\delta}U[x_k, P_K + \delta Q_K]|_{\delta=0} + \frac{d}{d\delta}\varepsilon^{elect}[x_k, P_K + \delta Q_K]|_{\delta=0} \\
&= 0
\end{aligned} \tag{13}$$

Physically, the variation of polarization P_K should result in the change of p_k, e_k, d_k, E_K, D_K, and ϕ because of the Maxwell equations and the pull back relationships (3)-(5). This implies that the variation Q_K results in:

$$\begin{aligned}
&p_k \to p_k + \delta\tilde{p}_k + o(\delta), \qquad \phi \to \phi + \delta\tilde{\phi} + o(\delta), \\
&e_k \to e_k + \delta\tilde{e}_k + o(\delta), \qquad d_k \to d_k + \delta d_k + o(\delta), \\
&E_K \to E_K + \delta\tilde{E}_K + o(\delta), \qquad D_K \to D_K + \delta D_K + o(\delta).
\end{aligned}$$

Furthermore, the following equations are valid for their leading order terms $\tilde{p}_k$, $\tilde{e}_k$, $\tilde{d}_k$, $\tilde{E}_K$, $\tilde{D}_K$ and $\tilde{\phi}$:

$$\begin{aligned}
&\tilde{d}_k = \epsilon_0\tilde{e}_k + \tilde{p}_k, \qquad \tilde{d}_{k,k} = 0, \\
&\tilde{p}_k = J^{-1}\alpha_{kK}Q_K, \qquad \tilde{E}_K = \tilde{e}_k x_{k,K}, \\
&\tilde{D}_K = JX_{K,k}\tilde{d}_k, \qquad \tilde{e}_k = \tilde{\phi}_{,k}.
\end{aligned}$$

Using divergence theorem, we can rewrite the first term in the RHS of (13) in the following form

$$\frac{d}{d\delta}U[x_k, P_K+\delta Q_K]|_{\delta=0} = \int_{\Omega_R}[\frac{\partial\psi}{\partial P_K}-(\frac{\partial\psi}{\partial\Pi_{KL}})_{,L}]Q_K dV+\int_{\partial\Omega_R}\frac{\partial\psi}{\partial\Pi_{KL}}Q_K N_L dA \tag{14}$$

where N_L represents the normal vector of the boundary $\partial\Omega_R$.

The Dirichlet boundary Γ_D, where the electric potential is specified, is the boundary for both Ω_R and V_R^*. By divergence theorem, the second term in the RHS of (13), the variation of electric energy, can be written as

$$\begin{aligned}
\frac{d}{d\delta}\varepsilon^{elect}[x_k, P_K+\delta Q_K]|_{\delta=0} &= \int_{\Omega+V*}(\epsilon_0 e_k\tilde{e}_k)dv + \int_{\Gamma_D}\phi_b N_K\tilde{D}_K dA \\
&= \int_{\Omega+V^*}(\epsilon_0 e_k\tilde{e}_k)dv + \int_{\Omega_R+V_R^*}(\phi\tilde{D}_K)_{,K}dV \\
&= \int_{\Omega+V^*}(\epsilon_0 e_k\tilde{e}_k)dv + \int_{\Omega+V^*}(\phi\tilde{d}_k)_{,k}dv \\
&= \int_{\Omega+V*}(-e_k\tilde{p}_k)dv \\
&= \int_{\Omega}(-e_k\tilde{p}_k)dv \\
&= \int_{\Omega_R}(-X_{L,k}E_L\alpha_{kK}Q_K)dV.
\end{aligned} \tag{15}$$

Then the first Euler-Lagrange equation and the associated boundary conditions can be obtained by substituting (14) and (15) into (13)

$$\begin{cases} \frac{\partial\psi}{\partial P_K} - (\frac{\partial\psi}{\partial\Pi_{KL}})_{,L} - X_{L,k}E_L\alpha_{kK} = 0 & \text{in } \Omega_R \\ \frac{\partial\psi}{\partial\Pi_{KL}}N_L = 0 & \text{on } \partial\Omega_R \end{cases} \tag{16}$$

Now we consider the variation of deformation (12). The variational calculations for this case lead to

$$\begin{aligned}
\frac{d}{d\delta}F[x_k+\delta u_k, P_K]|_{\delta=0} = \frac{d}{d\delta}U[x_k+\delta u_k, P_K]|_{\delta=0} + \frac{d}{d\delta}\varepsilon^{elect}[x_k+\delta u_k, P_K]|_{\delta=0} \\
+\frac{d}{d\delta}P^{mech}[x_k+\delta u_k]|_{\delta=0} = 0
\end{aligned} \tag{17}$$

Associated with the variation (12), there will also be changes for F_{kK}, G_{kKL}, J and F^{-1}_{Kk}

$$\begin{aligned}
&F_{kK} \to F_{kK} + \delta\tilde{F}_{kK}, \qquad G_{kKL} \to G_{kKL} + \delta\tilde{G}_{kKL}, \\
&J \to J + \delta\tilde{J} + o(\delta), \qquad F^{-1}_{Kk} \to F^{-1}_{Kk} + \delta\tilde{F^{-1}}_{Kk} + o(\delta).
\end{aligned}$$

Their leading terms are given by

$$\tilde{F}_{kK} = u_{k,K}, \qquad \tilde{G}_{kKL} = u_{k,KL},$$
$$\tilde{J} = JX_{K,k}u_{k,K}, \qquad \tilde{F^{-1}}_{kK} = -X_{L,k}X_{K,l}u_{l,L}. \tag{18}$$

We note that the reference quantities P_K, E_K, and D_K do not change with the variation u_k. However, the current quantities p_k, e_k and d_k are affected by the variation of u_k because of the equations (4). For this reason, it is simpler to use P_K, E_K and D_K in the variational calculations.

Using the divergence theorem, we first rewrite the internal energy into the following form

$$\frac{d}{d\delta}U[x_k + \delta u_k, P_K]|_{\delta=0} = \int_{\Omega_R} -[\frac{\partial \psi}{\partial x_{k,K}} - (\frac{\partial \psi}{\partial x_{k,KL}})_{,L}]_{,K}u_k dV$$
$$+ \int_{\partial\Omega_R}[\frac{\partial \psi}{\partial x_{k,K}} - (\frac{\partial \psi}{\partial x_{k,KL}})_{,L}]u_k N_K dA + \int_{\partial\Omega_R}\frac{\partial \psi}{\partial x_{k,KL}}u_{k,K}N_L dA \tag{19}$$

It is important to note that, in equation(19), the tangential component of $u_{k,K}$ is independent of u_k due to the constraint

$$\int_{\partial\Omega_R} V_{K,L}(\delta_{KL} - N_L N_K)dA = 0$$

for any vector V_K on the closed boundary $\partial\Omega_R$, where $\delta_{KL} = \mathbf{I}_K \cdot \mathbf{I}_L$ is the Kronecker delta which is nonzero only if $K = L$. The term $V_{K,L}(\delta_{KL} - N_L N_K)$ may also be viewed as a surface divergence of an arbitrary vector V_K on the boundary $\partial\Omega_R$.

The last integral on the rhs of (19) can be rewritten as:

$$\int_{\partial\Omega_R}[\frac{\partial \psi}{\partial x_{k,KL}}N_L(\delta_{KI} - N_K N_I)u_{k,I} + \frac{\partial \psi}{\partial x_{k,KL}}N_L N_K N_I u_{k,I}]dV$$
$$= \int_{\partial\Omega_R}\{[\frac{\partial \psi}{\partial x_{k,KL}}u_k N_L(\delta_{KI} - N_K N_I)]_{,I} - [\frac{\partial \psi}{\partial x_{k,KL}}N_L(\delta_{KI} - N_K N_I)]_{,I}u_k$$
$$+\frac{\partial \psi}{\partial x_{k,KL}}N_L N_K N_I u_{k,I}\}dV$$

where $\frac{\partial \psi}{\partial x_{k,KL}}u_k N_L(\delta_{KI} - N_K N_I)$ is a tangent vector on $\partial\Omega_R$ since $\frac{\partial \psi}{\partial x_{k,KL}}u_k N_L(\delta_{KI} - N_K N_I)N_I = 0$. Thus the divergence of this tangential vector is equal to its surface divergence. In other word, the integral $\int_{\partial\Omega_R}[\frac{\partial \psi}{\partial x_{k,KL}}u_k N_L(\delta_{KI} - N_K N_I)]_{,I}$ is zero.

Let $V_{kI} = \frac{\partial \psi}{\partial x_{k,KL}} N_L(\delta_{KI} - N_K N_I)$, then the equation (19) can be expressed as the following form

$$\begin{aligned}
&\frac{d}{d\delta} U[x_k + \delta u_k, P_K]|_{\delta=0} = \int_{\Omega_R} -[\frac{\partial \psi}{\partial x_{k,K}} - (\frac{\partial \psi}{\partial x_{k,KL}})_{,L}]_{,K} u_k dV \\
&+ \int_{\partial\Omega_R} \{[\frac{\partial \psi}{\partial x_{k,K}} - (\frac{\partial \psi}{\partial x_{k,KL}})_{,L}] N_K - V_{kI,I}\} u_k dA \\
&+ \int_{\partial\Omega_R} \frac{\partial \psi}{\partial x_{k,KL}} N_L N_K N_I u_{k,I} dA. \qquad (20)
\end{aligned}$$

Similar treatment of the higher order boundary terms may be found in Liu[54] and Yurkov.[55]

To do the variational calculus for the electric energy ε^{elect}, by divergence theorem, we first rewrite it in the following form:

$$\begin{aligned}
\varepsilon^{elect}[x_k, P_K] &= \int_{\Omega+V^*} \frac{\epsilon_0}{2} e_k e_k dv + \int_{\Gamma_D} \phi_b N_K D_K dA \\
&= \int_{\Omega+V^*} (\frac{\epsilon_0}{2} e_k e_k - e_k d_k) dv \\
&= \int_{\Omega_R+V_R^*} [\frac{\epsilon_0}{2} J X_{K,k} X_{L,k} E_K E_L - J X_{K,k} E_K (\epsilon_0 X_{L,k} E_L + J^{-1} \alpha_{kL} P_L)] dV \\
&= \int_{\Omega_R+V_R^*} [-\frac{\epsilon_0}{2} J X_{K,k} X_{L,k} E_K E_L - X_{K,k} \alpha_{kL} E_K P_L] dV
\end{aligned}$$

Using the relations in (18), we obtain the following form for the variation of electric field energy

$$\begin{aligned}
&\frac{d}{d\delta} \varepsilon^{elect}[x_k + \delta u_k, P_K]|_{\delta=0} \\
&= \int_{\Omega_R+V_R^*} [-\frac{\epsilon_0}{2} J X_{K,k} u_{k,K} (X_{L,l} X_{M,l} E_L E_M) + X_{K,l} u_{k,K} (\epsilon_0 J X_{L,k} X_{M,l} E_L E_M \\
&+ X_{L,k} \alpha_{lM} E_L P_M)] dV \\
&= \int_{\Omega_R+V_R^*} [-\frac{\epsilon_0}{2} J X_{K,k} u_{k,K} (X_{L,l} X_{M,l} E_L E_M) + u_{k,K} X_{L,k} E_L D_K] dV \\
&= -\int_{\Omega_R} [-\frac{\epsilon_0}{2} J X_{K,k} (X_{L,l} X_{M,l} E_L E_M) + X_{L,k} E_L D_K]_{,K} u_k dV + \\
&\int_{\partial\Omega_R} [-\frac{\epsilon_0}{2} J X_{K,k} (X_{L,l} X_{M,l} E_L E_M) + X_{L,k} E_L D_K] u_k N_K dA \\
&- \int_{V_R^*} [-\frac{\epsilon_0}{2} J X_{K,k} (X_{L,l} X_{M,l} E_L E_M) + X_{L,k} E_L E_K]_{,K} u_k dV. \qquad (21)
\end{aligned}$$

Let

$$\tilde{\Sigma}^{MW}_{kK} = -\frac{\epsilon_0}{2} J X_{K,k}(X_{L,l}X_{M,l}E_L E_M) + E_L X_{L,k} D_K \tag{22}$$

which is related to the Maxwell stress expression defined in current configuration[52,53]

$$\sigma^{MW}_{kl} = e_k d_l - \frac{\epsilon_0}{2} e_i e_i \delta_{kl} \tag{23}$$

by

$$\Sigma^{MW}_{kK} = J X_{K,l} \sigma^{MW}_{kl}.$$

Subsequently, we refer to Σ^{MW}_{kK} as the Piola-Maxwell stress.

Note that the polarization P_K vanishes in vacuum. Thus the two Maxwell stresses reduce to

$$\tilde{\Sigma}^{MW}_{kK} = -\frac{\epsilon_0}{2} J X_{K,k}(X_{L,l}X_{M,l}E_L E_M) + E_L X_{L,k} E_K$$

and

$$\sigma^{MW}_{kl} = e_k e_l - \frac{\epsilon_0}{2} e_i e_i \delta_{kl}$$

in the surrounding vacuum.

By substituting (20), (21), and (22) into (17), we have the second Euler-Lagrange equation and the associated boundary conditions

$$\begin{cases} [\frac{\partial \psi}{\partial x_{k,K}} - (\frac{\partial \psi}{\partial x_{k,KL}})_{,L} + \Sigma^{MW}_{kK}]_{,K} + B^e_K \alpha_{Kk} = 0 & \text{in } \Omega_R \\ \tilde{\Sigma}^{MW}_{kK,K} = 0 & \text{in } V* \\ [\frac{\partial \psi}{\partial x_{k,K}} - (\frac{\partial \psi}{\partial x_{k,KL}})_{,L} + \Sigma^{MW}_{kK}]N_K = V_{kI,I} + t^e_K \alpha_{Kk} & \text{on } \partial\Omega_R \\ \frac{\partial \psi}{\partial x_{k,KL}} N_K N_L = 0 & \text{on } \partial\Omega_R \end{cases} \tag{24}$$

In summary, in equilibrium, the electroelastic system should satisfy the following governing equations

$$\begin{cases} \frac{\partial \psi}{\partial P_K} - (\frac{\partial \psi}{\partial \Pi_{KL}})_{,L} - X_{L,k} E_L \alpha_{kK} = 0 & \text{in } \Omega_R \\ [\frac{\partial \psi}{\partial x_{k,K}} - (\frac{\partial \psi}{\partial x_{k,KL}})_{,L} + \Sigma^{MW}_{kK}]_{,K} + B^e_K \alpha_{Kk} = 0 & \text{in } \Omega_R \\ \tilde{\Sigma}^{MW}_{kK,K} = 0 & \text{in } V* \\ D_{K,K} = \rho^e_0 & \text{in } \Omega_R \end{cases} \tag{25}$$

and the boundary conditions

$$\begin{cases} \frac{\partial \psi}{\partial \Pi_{KL}} N_L = 0 & \text{on } \partial\Omega_R \\ [\frac{\partial \psi}{\partial x_{k,K}} - (\frac{\partial \psi}{\partial x_{k,KL}})_{,L} + \Sigma^{MW}_{kK}]N_K = V_{kI,I} + t^e_K \alpha_{Kk} & \text{on } \partial\Omega_R \\ \frac{\partial \psi}{\partial x_{k,KL}} N_K N_L = 0 & \text{on } \partial\Omega_R \end{cases} \tag{26}$$

2.5. *Internal energy density*

To model flexoelectricity, we consider the coupling between strain gradient and polarization as well as the coupling between polarization gradient and strain in the definition of the internal energy density.

The internal energy density $\psi(x_{k,K}, G_{k,KL}, P_K, \Pi_{KL})$ must be invariant under rigid translations and rotations. By Cauchy's theorem, the dependency of ψ on $x_{k,K}$ should be replaced by the dependency on $C_{KL} = x_{k,K}x_{k,L}$. It is also convenient to use the following strain tensor

$$S_{KL} = \frac{1}{2}(C_{KL} - \delta_{KL})$$

instead of C_{KL}. Thus $\frac{\partial \psi}{\partial x_{k,K}}$ is always written as $\frac{\partial \psi}{\partial S_{KL}} x_{k,L}$ using the chain rule.

We will reconsider nonlinearities in Section 7 when we address soft materials. Until Section 7, we assume small strains, keep only the leading order terms in the internal energy density and ignore the difference between the reference and the current configurations. In that case, the internal energy is given by

$$\begin{aligned}\psi(S_{kl}, G_{k,lm}, P_k, \Pi_{kl}) = &\frac{1}{2}a_{kl}P_kP_l + \frac{1}{2}b_{klmn}\Pi_{kl}\Pi_{mn} + \frac{1}{2}c_{klmn}S_{kl}S_{mn} \\ &+\frac{1}{2}d_{ijklmn}G_{ijk}G_{lmn} + e_{klmn}S_{kl}\Pi_{mn} \\ &+f_{klmn}P_kG_{lmn} + g_{klm}P_k\Pi_{lm} + h_{klm}P_kS_{lm} \quad (27)\end{aligned}$$

where the second order tensor a_{kl} is the reciprocal dielectric susceptibility, the fourth order tensor b_{klmn} is the polarization gradient-polarization gradient coupling tensor and c_{klmn} is the elastic tensor, the sixth order tensor d_{ijklmn} strain gradient-strain gradient coupling tensor, the fourth order tensor e_{klmn} corresponds to polarization gradient and strain coupling introduced by Mindlin,[56] whereas f_{klmn} is the fourth order flexoelectric tensor, h_{klm} and g_{klm} are the third order piezoelectric tensor and the polarization-polarization gradient coupling tensor, respectively.

3. Piezoelectric Thin Film Super Lattices Without Using Piezoelectric Materials

Consider a composite consisting of two or more different nonpiezoelectric dielectric materials. Even under the application of uniform stress, differences in material properties will result in the presence of strain gradients around the interfaces. Those strain gradients will induce polarization due to the

flexoelectric effect. For "properly designed"composites,[18] the net average polarization will be nonzero. Thus, the nanostructure will exhibit an overall electromechanical coupling under uniform stress behaving like a piezoelectric material. The individual constituents must be at the nanoscale since this concept requires very large strain gradients and those are generated easily only at the nanoscale.

Within the assumption of the linearized theory for centrosymmetric dielectrics, the internal energy density ψ can be assumed to be quadratic function of terms involving small strain S_{ij}, polarization P_i, polarization gradient $P_{i,j}$, and strain gradient $u_{i,jk}$

$$\begin{aligned}\psi(e_{ij}, P_i, P_{i,j}, u_{i,jk}) = \frac{1}{2}a_{kl}P_kP_l + \frac{1}{2}b_{ijkl}P_{i,j}P_{k,l} + \frac{1}{2}c_{ijkl}S_{ij}S_{kl},\\ + d_{ijkl}P_{i,j}S_{kl} + f_{ijkl}P_iu_{j,kl},\end{aligned} \tag{28}$$

Usually we must consider another term $\frac{1}{2}g_{ijklmn}u_{i,jk}u_{l,mn}$ in the internal energy form (28) to ensure the thermodynamic stability of the system.[18,19,27] This extra term represents purely nonlocal elastic effects and corresponds to the so-called strain gradient elasticity theories (see also Mao and Purohit[57]). However, the contribution of this term is small for the current problem.[19] There is no qualitative change to the effective piezoelectricity with the consideration of this term and the system studied here does not lose its stability when we exclude it.[18,19]

For a thin film structure the fields vary only in the thickness direction. Let x_1 be the thickness direction. After substituting (28) in the governing equation $(25)_{1,2,4}$, we obtain the following 1D governing equations for a single layer structure:

$$\begin{cases} c\frac{\partial^2 u}{\partial x_1^2} + (d-f)\frac{\partial^2 P}{\partial x_1^2} = 0, \\ (d-f)\frac{\partial^2 u}{\partial x_1^2} + b\frac{\partial^2 P}{\partial x_1^2} - aP - \frac{\partial \phi}{\partial x_1} = 0, \\ -\epsilon_0\frac{\partial^2 \phi}{\partial x_1^2} + \frac{\partial P}{\partial x_1} = 0. \end{cases} \tag{29}$$

Under open-circuit conditions, the electric displacement is zero

$$-\epsilon_0\frac{\partial \phi}{\partial x_1} + P = 0.$$

We arrive at the following equations

$$\frac{bc-(d-f)^2}{c}\frac{\partial^2 P}{\partial x_1^2} - (a+\epsilon_0^{-1})P = 0 \Rightarrow \frac{\partial^2 P}{\partial x_1^2} - \frac{P}{l^2} = 0, \tag{30}$$

where

$$l^2 = \frac{[bc-(d-f)^2]\epsilon_0}{c\eta} \text{ and } \eta = (1+a\epsilon_0).$$

Solving equation (30) for polarization, we obtain:

$$P = A_1 e^{-x_1/l} + A_2 e^{x_1/l}, \tag{31}$$

The displacement field is

$$u = A_3 + A_4 x_1 - \frac{d-f}{c} e^{-x_1/l}(A_1 + A_2 e^{2x_1/l}). \tag{32}$$

A_1,A_2,A_3, and A_4 are the constants of integration which may be determined by the boundary conditions. Since the coefficients d and f appear together, for conciseness, we write h instead of $(d-f)$.

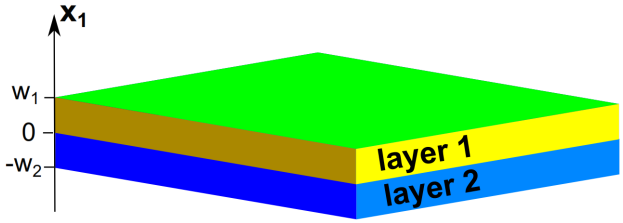

Fig. 5. A bilayer film composed of two different dielectric materials.

For the bilayer film shown in Fig. 5, its polarization and displacement fields for each layer are given by

$$\begin{cases} P_i = A_{i1}\exp(-\frac{x_1}{l_i}) + A_{i2}\exp(\frac{x_1}{l_i}), \\ u_i = A_{i3} + A_{i4}x_1 - \frac{h_i}{c_i}\exp(-\frac{x_1}{l_i})[A_{i1} + A_{i2}\exp(\frac{2x_1}{l_i})]. \end{cases} \tag{33}$$

where $i = 1, 2$ correspond to "layer 1"and "layer 2"shown in Fig. 5. The 8 constants of integration are determined by the following boundary conditions:

(1) Applied stress boundary conditions

$$(c_i \partial_{x_1} u_i + h_i \partial_{x_1} P_i) = \sigma.$$

(2) Continuity of stress at the interface

$$[\![\sigma]\!] = (\sigma^{(1)}|_{x_1\to 0} - \sigma^{(2)}|_{x_1\to 0}) = 0.$$

This condition is redundant, since in this case, the previous two (applied stress) conditions trivially ensure this continuity.

(3) Displacements at the interface are zero

$$u_i|_{x_1\to 0} = 0.$$

(4) Electric tensor (conjugate to the polarization gradient) $\Lambda_{ij} = \frac{\partial \psi}{\partial P_{i,j}}$ is set to zero at the free boundaries

$$\Lambda_{ij}^{(1)} = (d_i \partial_{x_1} u_i + b_i \partial_{x_1} P_i)|_{x_1 \to w_i} = 0.$$

(5) The electric tensor is specified to be continuous (but not necessarily zero) at the interface

$$[\![\Lambda_{ij}]\!]|_{x_1\to 0} = (\Lambda_{ij}^{(1)}|_{x_1\to 0} - \Lambda_{ij}^{(2)}|_{x_1\to 0}) = 0.$$

(6) Polarization (P) is specified to be continuous at the interface

$$[\![P]\!]|_{x_1\to 0} = (P_1|_{x_1\to 0} - P_2|_{x_1\to 0}) = 0.$$

Unlike classical theory of piezoelectricity, an additional boundary condition is required at the interface on the polarization field in order to avoid the singularities of polarization gradient field.

Finally, the following results are obtained:

$$\begin{aligned} P_1 &= \frac{A_1 + B_1}{C_1}, \\ P_2 &= \frac{A_2 + B_2}{C_2}, \end{aligned} \tag{34}$$

where

$$\begin{aligned} A_1 &= \sigma\epsilon_0 cosh(\frac{x_1 - w_1}{l_1})[-1 + cosh(\frac{w_2}{l_2})]c_1 h_2 l_1 \eta_1, \\ B_1 &= \sigma\epsilon_0 c_2 h_1 \{[cosh(\frac{x_1}{l_1}) - cosh(\frac{x_1 - w_1}{l_1})]cosh(\frac{w_2}{l_2}) l_1\eta_1 + \\ &\quad sinh(\frac{x_1}{l_1})sinh(\frac{w_2}{l_2}) l_2\eta_2\}, \\ C_1 &= c_1 c_2 l_1\eta_1[cosh(\frac{w_2}{l_2})sinh(\frac{w_1}{l_1})l_1\eta_1 + cosh(\frac{w_1}{l_1})sinh(\frac{w_2}{l_2})l_2\eta_2], \\ A_2 &= \sigma\epsilon_0 cosh(\frac{x_1 + w_2}{l_2})[-1 + cosh(\frac{w_1}{l_1})]c_2 h_1 l_2 \eta_2, \\ B_2 &= \sigma\epsilon_0 c_1 h_2 \{[cosh(\frac{x_1}{l_2}) - cosh(\frac{x_1 + w_2}{l_2})]cosh(\frac{w_1}{l_1}) l_2\eta_2 - \\ &\quad sinh(\frac{x_1}{l_2})sinh(\frac{w_1}{l_1}) l_1\eta_1\}, \\ C_2 &= c_1 c_2 l_2\eta_2[cosh(\frac{w_2}{l_2})sinh(\frac{w_1}{l_1})l_1\eta_1 + cosh(\frac{w_1}{l_1})sinh(\frac{w_2}{l_2})l_2\eta_2]. \end{aligned}$$

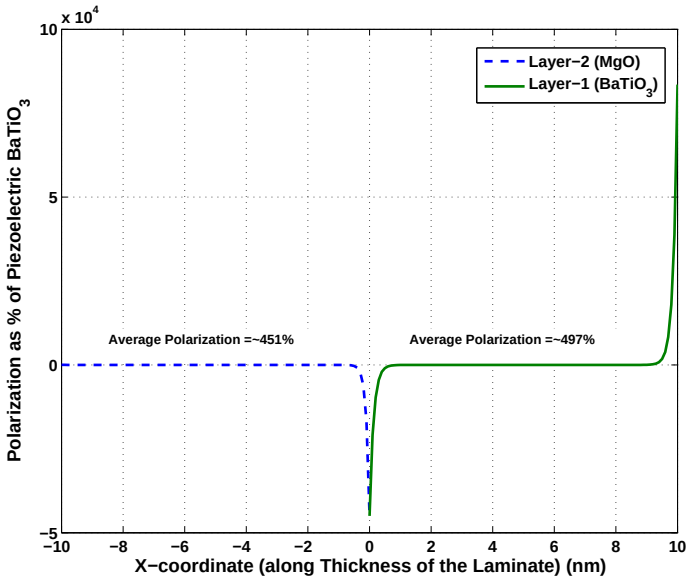

Fig. 6. Polarization distribution in each layer of a MgO-$BaTiO_3$ finite bilayer. Total average polarization in the bilayer is 23% of piezoelectric $BaTiO_3$. Reprinted with permission from AIP Publishing LLC.[18] Copyright 2010.

Numerical results for $BaTiO_3$-MgO bilayer are shown in Fig. 6. The calculated polarization is divided by the applied stress σ and then normalized by the piezoelectricity p_{33} of $BaTiO_3$ which is equal to $7.8\times10^{-11}C/N$. For these results, we assume both layers, layer-2(MgO) and Layer-1($BaTiO_3$) to be $10nm$ thick subject to a unit applied stress.

The material constants used in the above calculation are listed in the following table:

Table 1. Material properties for $BaTiO_3$ and MgO.

	$BaTiO_3$	MgO
$a_{11}(Nm^2/C^2)$	2.824×10^7	1.298×10^{10}
$b_{11}(Nm^4/C^2)$	6.77×10^{-6}	5.67×10^{-8}
$c_{11}(N/m^2)$	1.62×10^{11}	3.00×10^{11}
$h_{11}(Nm/C)$	-1.55×10^5	1.29×10^2
$l(\mathring{A})$	1.30	1.00

To find the effective piezoelectricity of this bilayer structure, we first calculate its average polarization $\bar{P}$ as follows:

$$\bar{P} = \frac{1}{w_1 + w_2}(\int_0^{w_1} P_1 dx_1 + \int_{-w_2}^{0} P_2 dx_1) = \frac{\bar{A}\bar{B}}{\bar{C}}, \tag{35}$$

where

$$\bar{A} = 4\sigma sinh(\frac{w_1}{2l_1})sinh(\frac{w_2}{2l_2})\epsilon_0(\eta_1 - \eta_2),$$
$$\bar{B} = cosh(\frac{w_1}{2l_1})sinh(\frac{w_2}{2l_2})c_1h_2l_1\eta_1 + cosh(\frac{w_2}{2l_2})sinh(\frac{w_1}{2l_1})c_2h_1l_2\eta_2,$$
$$\bar{C} = c_1c_2(w_1 + w_2)\eta_1\eta_2[cosh(\frac{w_2}{l_2})sinh(\frac{w_1}{l_1})l_1\eta_1 + cosh(\frac{w_1}{l_1})sinh(\frac{w_2}{l_2})l_2\eta_2].$$

Then the effective piezoelectricity d^{eff} is defined as $\bar{P}/\sigma$. We note that d^{eff} directly depends on the difference between the dielectric constants of the constituent materials. Larger dielectric contrast between the two layers will lead to a larger apparent piezoelectric coefficient. As shown in Fig. 6, the effective piezoelectricity for the present MgO-$BaTiO_3$ bilayer structure is 23% of that of $BaTiO_3$

4. Compression of a Truncated Cone, Effective Piezoelectric Response and Determination of Material Properties

The solution for the compression response of a truncated cone is an important case-study. Cross[1] profitably used this notion to show that such a geometrically graded structure behaves like an apparent piezoelectric material since even a uniform stress (e.g. compression) will result in an inhomogeneous strain and hence, due to flexoelectricity, produce a non-zero average polarization. Conversely, the solution to this problem also allows a facile way to experimentally estimate the flexoelectric properties of a material. We remark here that the the expression used by Cross and co-workers (although physically intuitive) is but a crude approximation which can lead to rather large errors—recent computational work by Abdollahi et. al.[58] attests to this. An exact solution to this problem is not possible and in this section we provide a perturbative calculation (which is an improvement) over what has been used in the past.[1]

As shown in Fig. 7, when the force F is applied to the top surface of the truncated cone, due to flexoelectricity, a current will flow through the circuit. Obviously, this is a 3D problem since the cross section changes with the coordinate x_1. However, the problem can be easily converted to a 1D problem if we assume that (1) after deformation, the displacement

u and polarization P are both in x_1 direction and (2) u and P only vary with the coordinate x_1. These two assumptions lead to the following consequences: (1) $S_{11} = du/dx_1$ is the only nonzero strain, (2) $u_{,11} = d^2u/dx_1^2$ is the only nonzero strain gradient, (3) $P_{,1} = dP/dx_1$ is the only nonzero polarization gradient. In the current example, to emphasize flexoelectricity, the contribution of polarization gradient to the internal energy is ignored. We note that omitting the polarization gradient term does not alter the governing equations (although the boundary conditions do change). In this case, the high order electric boundary conditions are replaced by the high order stress boundary conditions. We also assume that the deformation is small so that there is no difference between the current and the reference configurations—this is a reasonable assumption for hard crystalline materials . The volume integration over the truncated cone, $\int_\Omega dv$, can be written into an 1D integration from 0 to L, $\int_0^L A(x)dx$, with $A(x)$ being the area of the cross section at $x_1 = x$.

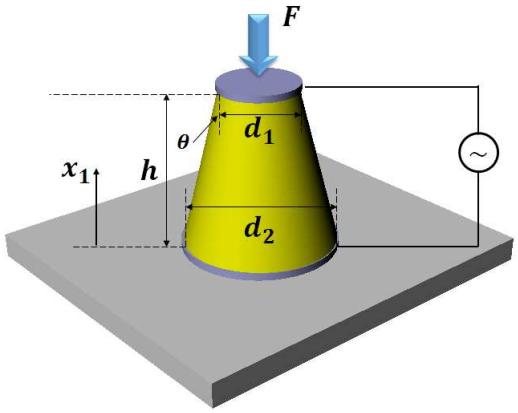

Fig. 7. A truncated cone under compression.

Based on the setup described above, the variations (14) and (15) become

$$\frac{d}{d\delta}U[\boldsymbol{\chi}, \mathbf{P}_\delta]|_{\delta=0} = \int_0^L A(x)\psi_P P_1 dx$$

and

$$\frac{d}{d\delta}\varepsilon^{elect}[\boldsymbol{\chi}, \mathbf{P}_\delta]|_{\delta=0} = \int_0^L A(x)(\frac{d\phi}{dx})P_1 dx.$$

Similarly, the variations (19) can be written into the following one dimensional form

$$\frac{d}{d\delta}U[\boldsymbol{\chi}_\delta, \mathbf{P}]|_{\delta=0} = \int_0^L \{-\frac{d}{dx}[A(x)\frac{\partial\psi}{\partial S_{11}}] + \frac{d^2}{dx^2}[A(x)\frac{\partial\psi}{\partial u_{,11}}]\}u_1 dx$$
$$+[A(x)\frac{\partial\psi}{\partial u_{,11}}]_{x=0\&L} + \{A(x)\frac{\partial\psi}{\partial S_{11}} - \frac{d}{dx}[A(x)\frac{\partial\psi}{\partial u_{,11}} - F]\}_{x=L}.$$

Because of the small deformation assumption, the variation (21) becomes zero so that the Maxwell stress vanishes. Then we have the Euler-Lagrange equations for this truncated cone

$$\begin{cases} \frac{d}{dx}[A(x)\frac{\partial\psi}{\partial S_{11}} - \frac{d}{dx}(A(x)\frac{\partial\psi}{\partial u_{,11}})] = 0 \\ \frac{\partial\psi}{\partial P} + \frac{d\phi}{dx} = 0 \end{cases} \tag{36}$$

and the associated boundary conditions

$$\begin{cases} \frac{\partial\psi}{\partial u_{,11}} = 0 & \text{at } x = 0 \text{ and } x = L \\ A(x)\frac{\partial\psi}{\partial S_{11}} - \frac{d}{dx}[A(x)\frac{\partial\psi}{\partial u_{,11}}] = F & \text{at } x = L \\ u = 0 & \text{at } x = 0. \end{cases} \tag{37}$$

Here we use a reduced version of the internal energy density

$$\psi = \frac{1}{2}aP^2 + \frac{1}{2}c(\frac{du}{dx})^2 + \frac{1}{2}g(\frac{d^2u}{dx^2})^2 + fP\frac{d^2u}{dx^2} \tag{38}$$

where the polarization gradient term is dropped. It is found that the governing equation remains unaltered without the consideration of this term due to the fact that[18]

$$\frac{dP}{dx}\frac{du}{dx} = \frac{d}{dx}(P\frac{du}{dx}) - P\frac{d^2u}{dx^2}$$

and $\frac{d}{dx}(P\frac{du}{dx})$ can be converted to a boundary term by divergence theorem.

Substituting (38) into the governing equations (36) and the associated boundary conditions (37), we obtain

$$\begin{cases} -gA(x)\frac{d^3u}{dx^3} - g\frac{dA(x)}{dx}\frac{d^2u}{dx^2} + cA(x)\frac{du}{dx} - fA(x)\frac{dP}{dx} - f\frac{dA(x)}{dx}P = F & \text{on } (0,h), \\ aP + f\frac{d^2u}{dx^2} + \frac{d\phi}{dx} = 0 & \text{on } (0,h), \\ \frac{d}{dx}[A(x)(-\frac{1}{\epsilon_0}\frac{d\phi}{dx} + P)] = 0 & \text{on } (0,h), \\ \frac{\partial\psi}{\partial u_{,11}} = g\frac{d^2u}{dx^2} + fP & \text{at } x = 0\&h, \\ u(0) = 0, \\ \phi(0) - \phi(h) = 0. \end{cases} \tag{39}$$

where $A(x) = \frac{\pi}{4}(d_2 - \frac{d_2-d_1}{h}x)^2$ denotes the cross section area at x. Note that if the half cone angle θ is very small, $a(x)$ can be approximately expressed as

$$A(x) = \pi\theta^2 x^2 + \bar{d}\theta x + a_2 \tag{40}$$

where $\bar{d} = -\pi d_2$ and $a_2 = \frac{\pi}{4}d_2^2$.

In the extreme case, when θ is zero, the truncated cone becomes a finite circular cylinder. Obviously, in that case, neglecting any edge effects, the flexoelectric response vanishes. Let $u_0(x)$ and $P_0(x)$ denote the solution for the cylinder problem. Then the solution for a truncated cone problem can be written as

$$\begin{cases} u(x) = u_0(x) + \theta u_1(x) + \theta^2 u_2(x) + ... \\ P(x) = P_0(x) + \theta P_1(x) + \theta^2 P_2(x) + ... \\ \phi(x) = \phi_0(x) + \theta\phi_1(x) + \theta^2\phi_2(x) + ... \end{cases} \tag{41}$$

Substitutng (40) and (41) into the governing equations and considering only zeroth order tens, we have the following equations for $u_0(x)$ and $P_0(x)$

$$\begin{cases} -g\frac{d^3u_0}{dx^3} + c\frac{du_0}{dx} - f\frac{dP_0}{dx} = F/a_2 & \text{on } (0,h), \\ aP_0 + f\frac{d^2u_0}{dx^2} + \frac{d\phi_0}{dx} = 0 & \text{on } (0,h), \\ -\epsilon_0\frac{d^2\phi_0}{dx^2} + \frac{dP_0}{dx} = 0 & \text{on } (0,h), \\ g\frac{d^2u_0}{dx^2} + fP_0 = 0 & \text{at } x = 0\&h, \\ u_0(0) = 0, \\ \phi_0(0) - \phi_0(h) = 0. \end{cases} \tag{42}$$

Unsurprisingly the solution for the zeroth order equations (the case corresponding to the cylinder) is

$$u_0(x) = \frac{F}{ca_2}x, \qquad \text{and} \qquad P_0(x) = \phi_0(x) = 0.$$

The first order equations are:

$$\begin{cases} g\frac{d^3u_1}{dx^3} - c\frac{du_1}{dx} + f\frac{dP_1}{dx} = \bar{d}F/a_2^2 x & \text{on } (0,h), \\ aP_1 + f\frac{d^2u_1}{dx^2} + \frac{d\phi_1}{dx} = 0 & \text{on } (0,h), \\ -\epsilon_0\frac{d^2\phi_1}{dx^2} + \frac{dP_1}{dx} = 0 & \text{on } (0,h), \\ g\frac{d^2u_1}{dx^2} + fP_1 = 0 & \text{at } x = 0\&h, \\ u_1(0) = 0, \\ \phi_1(0) - \phi_1(h) = 0. \end{cases} \tag{43}$$

From $(43)_3$, we have

$$\frac{d\phi}{dx} = \frac{1}{\epsilon_0}P_1 - \frac{C_1}{\epsilon_0} \tag{44}$$

where C_1 is the constant of integration. Substituting the relationship (44) into $(43)_2$, we can express the polarization P_1 in terms of the displacement u_1 as

$$P_1 = -\frac{f\epsilon_0}{a\epsilon_0+1}\frac{d^2u_1}{dx^2} + \frac{C_1}{a\epsilon_0+1}.$$

A nonhomogeneous ODE for $u_1(x)$ is obtained from $(43)_1$

$$(g - \frac{f^2\epsilon_0}{a\epsilon_0+1})\frac{d^3u_1}{dx^3} - c\frac{du_1}{dx} = \bar{d}F/a_2^2 x.$$

The solution for this ODE is given by

$$u_1 = A_1e^{-x/l} + A_2e^{x/l} - \frac{\bar{d}F}{2ca_2^2}x^2 + C_2 \tag{45}$$

where $l^2 = (g - \frac{f^2\epsilon_0}{a\epsilon_0+1})/c$ depends on the material properties, A_1, A_2, C_1, and C_2 are constants to be determined by the following four boundary conditions

$$\begin{cases} (A_1 + A_2) = -\frac{fC_1}{c(a\epsilon_0+1)} = m, \\ (A_1e^{-h/l} + A_2e^{h/l}) = -\frac{fC_1}{c(a\epsilon_0+1)} = m, \\ A_1 + A_2 + C_2 = 0, \\ 2(A_1 - A_2) + \frac{alh}{f}C_1 = \frac{\bar{d}Flh}{ca_2^2} \end{cases}$$

where the last equation originates from the short circuit condition $\phi_1(0) = \phi_1(h)$. The solution for these four equations is given by

$$\begin{cases} A_1 = m\frac{e^{2h/l} - e^{h/l}}{e^{2h/l}-1}, \\ A_2 = m\frac{e^{h/l}-1}{e^{2h/l}-1}, \\ C_1 = \frac{\bar{d}Flh}{ca_2^2}/[\frac{alh}{f} - \frac{2f}{c(a\epsilon_0+1)}\tanh\frac{h}{2l}], \\ C_2 = -m. \end{cases} \tag{46}$$

Finally, using the relationship between P_1 and u_1, the expression for P_1 can be obtained as

$$P_1 = -\frac{f\epsilon_0}{a\epsilon_0+1}[\frac{1}{l^2}(A_1e^{-x/l} + A_2) - \frac{\bar{d}F}{ca_2^2}] + \frac{C_1}{a\epsilon_0+1}. \tag{47}$$

As a simplification, if we set $A_1 = A_2 = 0$, then we have $C_2 = 0$ and $C_1 = \frac{\bar{d}Ff}{aca_2^2}$ by (46). It is also found from equation (45) that u_1 becomes a

quadratic function of x. This implies that the strain gradient d^2u_1/dx^2 is a constant. Thus the solution for P_1 reduces to

$$P_1 = \frac{f\epsilon_0}{a\epsilon_0 + 1}\frac{\bar{d}F}{ca_2^2} + \frac{C_1}{a\epsilon_0 + 1} = \frac{\bar{d}Ff}{aca_2^2}$$

and the overall polarization P takes the following form

$$P = P_0 + \theta P_1 = -2(\frac{d_2 - d_1}{d_2}\frac{d_1^2}{d_2^2})\frac{f}{ach}\frac{F}{a_1}$$

where $a_1 = \frac{\pi}{4}d_1^2$ is the cross-sectional area of the top surface where the external force F is applied. Since the flexoelectric coefficient $\mu = -\frac{f}{a}$ and the applied surface traction $t^e = \frac{F}{a_1}$, the polarization can be also written as

$$P = 2(\frac{d_2 - d_1}{d_2}\frac{d_1^2}{d_2^2})\frac{\mu}{ch}t^e.$$

Then the effective piezoelectric coefficient is given by

$$d^{eff} = \frac{\partial P}{\partial t^e} = 2(\frac{d_2 - d_1}{d_2}\frac{d_1^2}{d_2^2})\frac{\mu}{ch}. \tag{48}$$

This result is similar to that obtained in Cross's work[1] where an effective piezoelectric coefficient

$$d^{eff} = \mu\frac{\frac{d_2^2 - d_1^2}{d_1^2}}{ch}$$

is obtained for the truncated pyramid. Both cases show that d^{eff} is proportional to the flexoelectric coefficient μ and the reciprocals of elastic modulus c and the dimension h. A more sophisticated perturbation approach may be necessary to obtain an analytical result that matches the computational corrections shown by Abdollahi et. al.[58]

5. Flexoelectric Beam Bending, Vibration and Energy Harvesting

Bending a beam is perhaps the easiest way to induce strain gradients and invoke a flexoelectric response. This is also a the model problem when considering energy harvesting from mechanical vibrations. As shown in Fig. 8, in this section we consider a cantilever beam subjected to a distributed load. B, h and L correspond to the width, hight and length of the beam, respectively. $q(x_1)$ is the distributed loading applied to the beam.

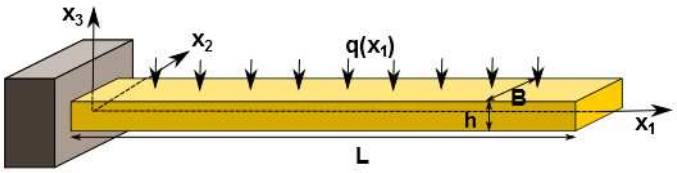

Fig. 8. A cantilever beam subjected to a distributed load.

To illustrate the central ideas of the flexoelectricity in this beam, we use the Euler-Bernoulli model. The key conclusions that we are interested in emphasizing in this work are unlikely to be affected by this assumption. The displacement field in the Euler-Bernoulli model is:

$$\mathbf{u} = \{-x_3 \frac{\partial w(x_1)}{\partial x_1}, 0, w(x_1)\}^T, \tag{49}$$

where $w(x_1)$ is the transverse displacement of the neutral surface at point x_1. From this displacement field, the normal strain in x_1 direction is the only non-zero strain component which is given by

$$S_{11} = -x_3 \frac{\partial^2 w}{\partial x_1^2}. \tag{50}$$

The non-zero strain gradient components are

$$S_{11,1} = -x_3 \frac{\partial^3 w(x_1)}{\partial x_1^3}, \qquad S_{11,3} = -\frac{\partial^2 w(x_1)}{\partial x_1^2}. \tag{51}$$

Since the thickness h of the beam is much smaller than its length L, it is found that $S_{11,1}$ is much smaller than $S_{11,3}$ for this Euler-Bernoulli beam problem. Therefore the component $S_{11,1}$ is ignored in the present work.

Generally, the strain gradient $S_{11,3}$ will induce the separation of positive and negative charge centers. A schematic representation for the polarization induced by strain gradient is given in Fig. 9. The blue and red particles represent the negative and positive charged material particles in a unit cell. As can be seen from Fig. 9, after deformation, the induced polarization is generated along the x_3 direction. The polarization density field within the cantilever beam has the following form:

$$\mathbf{P}(x_1, x_3) = \{0, 0, P(x_1, x_3)\}^T. \tag{52}$$

For this problem, the stored energy density ψ is given by

$$\begin{aligned} \psi &= \frac{1}{2} c S_{11}^2 + \frac{1}{2} g S_{11,3}^2 + \frac{1}{2} a P^2 + f S_{11,3} P \\ &= \frac{1}{2} c x_3^2 w_{,11}^2 + \frac{1}{2} g w_{,11}^2 + \frac{1}{2} a P^2 - f w_{,11} P \end{aligned} \tag{53}$$

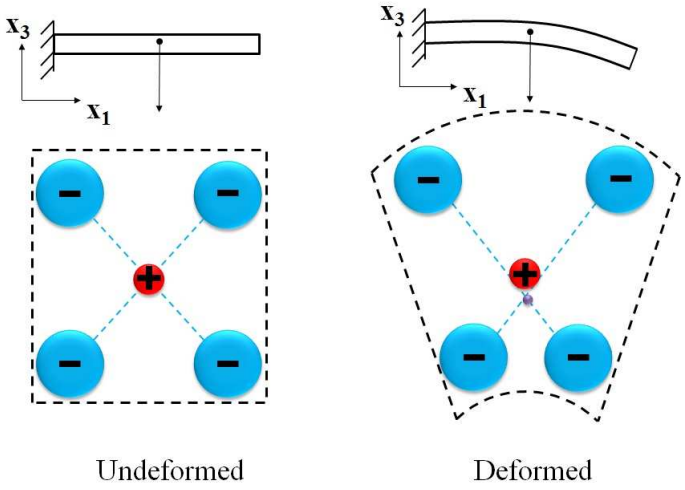

Fig. 9. Polarization due to bending of a centrosymmetric beam. Reprinted with permission from ELSEVIER.[59] Copyright 2014.

where $w_{,1}$ and $w_{,11}$ denote the 1st and 2nd order derivatives of w with respect to x_1, respectively; c, g, a, and f are material properties mentioned in section 2.

The so-called *dynamic* flexoelectric effect may strongly affect the electromechanical behavior of the sample at extremely high frequency vibrations.[24,46,47] However, in our current example, we have ignored this effect since the considered sample size is on the scale of microns and its natural frequency is still very low compare to that of the lattice vibration at which the dynamic flexoelectric effect is expected to play a role.

Once again, we stay within the linearized regime and ignore the distinction between current and reference configurations and the effect of Maxwell stress. Both these effects are important for soft materials but not for hard ones. Given these assumptions, the governing equations $(25)_{1,4}$ become

$$\begin{cases} aP - fw_{,11} + \phi_{,3} = 0 \\ -\epsilon_0 \phi_{,33} + P_{,3} = 0 \end{cases} \tag{54}$$

where $\phi_{,3} = -E$ is the derivative of potential ϕ with respect to x_3. From

(54), we further have

$$\begin{cases} P = \frac{f}{a} w_{,11} - \frac{1}{a}\phi_{,3}, \\ -(\epsilon_0 + \frac{1}{a})\phi_{,33} = 0. \end{cases} \tag{55}$$

With the applied boundary conditions for electric potential ϕ: $\phi(x_1, h/2) = V$ and $\phi(x_1, -h/2) = 0$, the leading order solutions of (55) are

$$\phi = \frac{V}{h} x_3 + \frac{V}{2}, \tag{56}$$

and

$$P = \frac{f}{a} w_{,11} - \frac{V}{h}. \tag{57}$$

Substituting (56) and (57) into (53) and integrating over the beam cross section, the following 1D energy density ψ_b is obtained

$$\psi_b = \int_A \psi da = \frac{1}{2} G_E w_{,11}^2 + \frac{AV^2}{2ah^2} \tag{58}$$

where $G_E = cI + gA - \frac{f^2 A}{a}$ and A denotes the cross-sectional area and I is the moment of inertia.

Free-energy minimization leads to the following equation:

$$\int_0^L \delta\psi_b dx_1 = \int_0^L G_E w_{,11} \delta w_{,11} dx_1 = \int_0^L q(x) \delta w dx_1$$

Using the divergence theorem, we obtain the following governing equation and boundary conditions:

$$\begin{cases} G_E \frac{\partial^4 w(x_1)}{\partial x_1^4} = q(x_1), \\ w(0) = \frac{\partial w(0)}{\partial x_1} = 0, \\ \frac{\partial^2 w(L)}{\partial x_1^2} = \frac{\partial^3 w(L)}{\partial x_1^3} = 0. \end{cases} \tag{59}$$

If the distributed load is a constant q_0, then the displacement w and polarization P are given by

$$w(x_1) = \frac{q_0}{24 G_E} x_1^4 - \frac{q_0 L}{6 G_E} x_1^3 - \frac{q_0}{2 G_E}(\frac{L^2}{2} - L) x_1^2, \tag{60}$$

$$P(x_1) = \frac{f}{a}[\frac{q_0}{2 G_E} x_1^2 - \frac{q_0 L}{G_E} x_1 - \frac{q_0}{G_E}(\frac{L^2}{2} - L)] - \frac{V}{ah}. \tag{61}$$

As shown in (61), because of flexoelectricity, both V and q_0 contribute to the polarization P. The former is due to the electric field while the latter is the result of flexoelectricity.

The example problem discussed in the preceding paragraphs shows that the bending of a dielectric beam will induce the net polarization because of flexoelectricity. One of the applications of this phenomena is energy harvesting. A proposed flexoelectric energy harvester is shown in Fig. 10. The cantilever beam is mounted to a base moving in x_3 direction. The transverse base displacement is denoted by $w_b(t)$. Due to the movement of the base, the cantilever beam undergoes bending vibrations. Dynamic strain gradient associated with vibration results in an alternating potential difference across the electrodes. The electrodes are connected to a resistive load (R) to quantify the electrical power output. Although the internal resistance of the dielectric beam is not taken into account, it can easily be considered as a resistor connected in parallel to the load resistance.

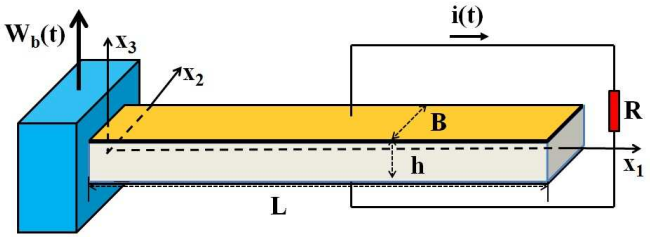

Fig. 10. A centrosymmetric flexoelectric energy harvester under base excitation. Reprinted with permission from ELSEVIER.[59] Copyright 2014.

For this vibration problem, the kinetic energy, which results in the inertial term in the governing equation, should be considered. In our recent paper,[59] from the following variational principle

$$\delta \int_{t_1}^{t_2} dt \int_V [\frac{1}{2}\rho \dot{u}_k \dot{u}_k - (\psi - \frac{1}{2}\epsilon_0 \phi_{,k}\phi_{,k} + P_k)]dV + \int_{t_1}^{t^2} dt \int_V (q_k \delta u_k + E_k^0 P_k)dV + \int_{t_1}^{t^2} dt \int_{\partial V} \tilde{D}\delta\phi dA = 0, \tag{62}$$

along with the Euler-Bernoulli beam assumption (49), we obtained the following equation

$$\int_{t_1}^{t^2} dt \int_0^L \rho A(\ddot{w} + \ddot{w}_b)\delta w dx_1 + \int_{t_1}^{t^2} dt \int_0^L (G_E \frac{\partial^2 w}{\partial x_1^2} - \frac{fA}{ah}V(t))\delta(\frac{\partial^2 w}{\partial x_1^2})dx_1 = 0. \tag{63}$$

The current $i(t)$ flows through the resistor R must be equal to the time rate of change of the average electric displacement $\tilde{D}_3 = \frac{1}{h}\int_V D_3 dV$, resulting the electric circuit equation with flexoelectric coupling

$$i(t) = \frac{V(t)}{R} = \frac{1}{h}\frac{d}{dt}\int_V (-\epsilon_0 \frac{V(t)}{h} + P) dV. \tag{64}$$

The governing equation (63) and (64) for variables $w(x)$ and $V(t)$ are numerically solved using the assumed-mode method.[60,61] The following finite series is used to represent the mechanical response of the beam:

$$w(x_1, t) = \sum_{k=1}^{N} a_k(t)\xi_k(x_1)$$

where N is the number of modes used in the series discretization, $\xi_k(x_1)$ are the kinematically admissible trial functions which satisfy the essential boundary conditions, while $a_k(t)$ are unknown generalized coordinates.

Since the focus in energy harvesting is placed on the resonance behavior (i.e. damping controlled region), it is necessary to account for structural dissipation in the system. In this work, we resort to Rayleigh damping which is proportional to the mass and the stiffness matrices. We introduce the damping matrix $\mathbf{D}$ with

$$\mathbf{D} = \mu\mathbf{M} + \gamma\mathbf{K}$$

where μ and γ are constants of proportionality which can be calculated using two modal damping ratios, ζ_1 and ζ_2 through the following equation:[62]

$$\begin{bmatrix}\gamma \\ \mu\end{bmatrix} = \frac{2\omega_1\omega_2}{\omega_1^2 - \omega_2^2}\begin{bmatrix}\frac{1}{\omega_2} & -\frac{1}{\omega_1} \\ -\omega_2 & \omega_1\end{bmatrix}\begin{bmatrix}\zeta_1 \\ \zeta_2\end{bmatrix}$$

where ω_1 and ω_2 are the first two nature frequencies of the beam. In the absence of other damping mechanisms, the damping ratio is related to the material quality factor ($Q = 1/2\zeta$).

Then the discrete Euler-Lagrange equations, duly considering Rayleigh damping, are given by

$$\mathbf{M}\ddot{\mathbf{a}}(t) + \mathbf{D}\dot{\mathbf{a}} + \mathbf{K}\mathbf{a} - \mathbf{\Theta}V(t) = \bar{\mathbf{f}}, C_f\dot{V}(t) + \frac{V(t)}{R} + \mathbf{\Theta}^T\dot{\mathbf{a}}(t) = 0 \tag{65}$$

where

$$
\begin{aligned}
M_{kl} &= \rho A \int_0^L \xi_k(x_1)\xi_l(x_1)dx_1, \\
K_{kl} &= G_E \int_0^L \xi_k''(x_1)\xi_l''(x_1)dx_1, \\
D_{kl} &= \mu M_{kl} + \gamma K_{kl}, \\
\Theta_l &= \frac{fA}{ah}\int_0^L \xi_l'' dx_1, \\
\bar{f}_l &= -\ddot{w}_b(t)\int_0^L \rho A \xi_l(x_1)dx_1, \\
C_f &= \frac{BL}{h}(\epsilon_0 + \frac{1}{a}).
\end{aligned}
$$

We choose polyvinylidene difluoride (PVDF) as the model material system which has the following properties: $a = \frac{1}{\epsilon - \epsilon_0} = 1.38 \times 10^{10} Nm^2/C^2$, $f = -a\mu_{12}' = -179Nm/C$ ($\mu_{12}' = 1.3 \times 10^{-10} C/m$ is the flexoelectric coefficient), $c = 3.7GPa$, $g = 5 \times 10^{-7} N$, and $\rho = 1.78 \times 10^3 kg/m^3$. To demonstrate the effect of scaling, here we explore the energy conversion efficiency of this flexoelectric energy harvester. The conversion efficiency is simply the ratio of the electrical power output to the mechanical power input, i.e. the power due to the shear force exerted on the beam by the base. The peak electrical power output is $|V(t)|^2/R$. The shear force exerted on the beam by the base is the shear force at $x_1 = 0$, which can be easily expressed by $cI\frac{d^3w(0)}{dx_1^3}$. Therefore the power due to the shear force is the product of the shear force and the base velocity $\frac{de_b(t)}{dt}$. Then the mechanical-to-electric energy conversion efficiency is

$$
\eta = \frac{|V(t)|^2/R}{|cI\frac{d^3w(0)}{dx_1^3}| \cdot |\frac{de_b(t)}{dt}|}.
$$

We maintain the shape of the sample (in terms of the aspect ratio, 100:10:1) and vary the thickness of the beam from $3\mu m$ through $0.3\mu m$. As shown in Fig. 11, for the 10 different sizes considered in this thickness range, the energy conversion efficiency monotonously increase as the decrease of the sample size. Specifically, the magnitude of the highest curve is about two orders higher than that of the lowest one. Further enhancement in the conversion efficiency can be expected as the beam thickness is reduced to nanometer scale.

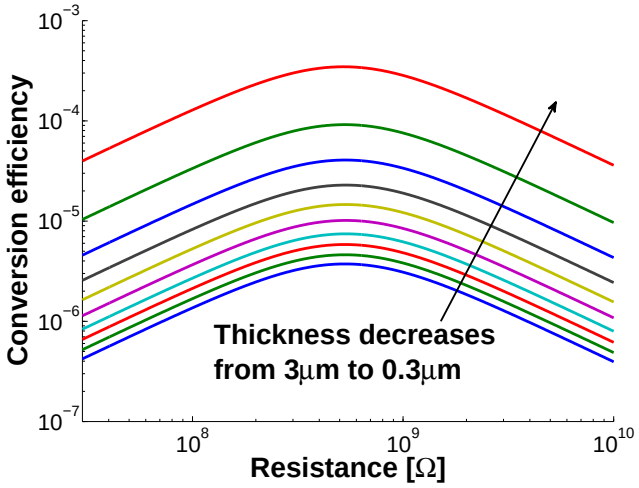

Fig. 11. Resonant energy conversion efficiency for different beam thickness levels (aspect ratio is the same: 100:10:1). Reprinted with permission from ELSEVIER.[59] Copyright 2014.

6. Flexoelectric Membranes

It is anticipated that the coupling between elasticity and electricity in biological membranes is important for many biological functions such as: ion transport,[63] mechanotransduction in outer hair cells,[64–66] tether formation.[67] It is also found that all the above mentioned biological phenomena are closely related to the flexoelectricity of the biomembranes. From a mechanistic viewpoint, we can rule out the piezoelectric effect in (most) biological membranes through symmetry arguments. Therefore, the leading order coupling between strain and polarization has to be 'flexoelectricity.

The flexoelectric theory of thin membranes has been developed in Mohammadi et. al.,[68] Qian et. al[43] and several other formal considerations are presented in Liu's paper.[54] In this formulation, we consider a thin membrane occupying $U \times (-h/2, h/2) \subset \mathbb{R}^3$, with $U \subset \mathbb{R}^2$ being an open bounded domain in the xy-plane and h being the thickness of the membrane. Since the thickness $h \ll 1$, the thin membrane may be idealized as a two-dimensional body; the thermodynamic state is then described by the out-of-plane displacement $w : U \to \mathbb{R}$ and the out-of-plane polarization $P : U \to \mathbb{R}$. For thin membrane, we also anticipate that bending is the predominant mode of deformation, and hence use the linearized curva-

ture tensor (or strain gradient) of the membrane $\kappa_{ij} = -w_{,ij}$ (for this two dimensional problem $i, j = 1, 2$) to describe the deformed state of the membrane. The polarization P is assumed to point along the normal direction throughout the deformation.

To model the flexoelectric effect, we postulate that the total internal/stored energy of an isotropic membrane is given by

$$U[w, P] = \int_U W(w_{,ij}, P), \tag{66}$$

where $W : \mathbb{R}^{2\times 2}_{sym} \times \mathbb{R} \to \mathbb{R}$ is the total internal energy density function and given by a quadratic function

$$W(w_{,ij}, P) = \frac{\kappa_b}{2}(w_{,ii})^2 + \kappa_g det(w_{,ij}) + fPw_{,ii} + \frac{1}{2}a_3P^2 \tag{67}$$

here we notice that the elastic part, $\frac{\kappa_b}{2}(w_{,ii})^2 + \kappa_g det(w_{,ij})$, of the membrane energy coincides with the linearized Helfrich-Canham model[69] of biological membranes that are widely used by bio-physicists (which is in turn identical to the Kirchhoff-Love plate theory), the term $fPw_{,ii}$ gives rise to the coupling between polarization and curvature (flexoelectric effects), and the last term $\frac{1}{2}a_3P^2$ arises from the dielectric property of the membrane. The constants κ_b, κ_g, f, and a_3 are material properties of the flexoelectric membrane and may in general depend on in-plane positions. Moreover, the stability of the membrane requires that:[68]

$$\kappa_b > 0, \qquad -2\kappa_b < \kappa_g < 0, \qquad a > 0, \qquad \text{and} \qquad \kappa_b + \frac{\kappa_g}{2} > \frac{f^2}{a} \tag{68}$$

The boundary of the flexoelectric membrane is clamped: $w, w_{,i}|_{\partial U} = 0$. Then under the application of an external electric field $E_3 : U \to \mathbb{R}$ and a mechanical body force $b_3 : U \to \mathbb{R}$, the total free energy of the membrane is given by

$$F[w, P] = \int_U W(w_{,ij}, P) - \int_U (PE_3 + wb_3), \tag{69}$$

where the first integral is the internal energy of the flexoelectric membrane, and the second one is the potential energy arising from the interaction between the membrane and the external electric field and mechanical loading device.

In the equilibrium state, by the principle of minimum free energy the pair of (w, P) shall minimize the total free energy (69):

$$\min_{(w,P)\in\mathcal{S}} F[w, P] \tag{70}$$

where the admissible space for (w, P) is given by

$$\mathcal{S} := \{(w, P) : \int_U |w_{,ij}|^2 < +\infty, \int_U |P|^2 < +\infty, w, w_{,i}|_{\partial U} = 0\} \tag{71}$$

By standard variational calculations, it can be shown that a minimizer (w, P) of the minimization problem (70) necessarily satisfies the following Euler-Lagrange equations and boundary conditions:

$$\begin{cases} (L_{ijkl} w_{,kl})_{,ij} + (fP)_{,ii} - b_3 = 0 & \text{on } U, \\ f w_{,ii} + aP - E_3 = 0 & \text{on } U, \\ w = 0, \quad w_{,i} = 0 & \text{on } \partial U \end{cases} \tag{72}$$

where L_{ijkl} $(i, j, k, l = 1, 2)$ represent the bending stiffness tensor which links the bending moment and the curvature of a membrane.

Using $(72)_2$ we eliminate P in $(72)_1$ and obtain

$$\begin{cases} [(L_{ijkl} - \frac{f^2}{a}\delta_{ij}\delta_{kl}) + \frac{f}{a}E_3\delta_{ij}]_{,ij} - b_3 = 0 & \text{on } U, \\ w = 0, \quad w_{,i} = 0 & \text{on } \partial U. \end{cases} \tag{73}$$

Consider a flexoelectric membrane. In the absence of applied body force $b_3 = 0$, the membrane can nevertheless be bent by an external electric field since the term $\frac{f}{a}E_3\delta_{ij}$ in $(73)_1$ serves as a "source" term for the boundary value problem (73) of w. It is of interest to investigate the effects of the external field on w. For simplicity, assume that the membrane is homogeneous and isotropic, and hence the boundary value problem can be rewritten as

$$[\kappa_b w_{kk} + \gamma E_3]_{,ii} = 0 \qquad \text{on } U, \tag{74}$$

where $\kappa_b = 2\mu_b + \lambda_b - (f^2/a)$ and $\gamma = f/a$. For appropriate boundary conditions as specified in $(73)_3$, it is standard to solve (74) for w. As examples, below we present a few explicit solutions, assuming infinite membrane on $\mathbb{R}^2$ and natural boundary conditions at the infinity:

$$|w_{,ij}(x_k)| \to 0 \qquad \text{as } x_k \to +\infty \tag{75}$$

We remark that w is only determined within an arbitrary linear function of (x_1, x_2) by the above conditions (75). Also, appropriate decay conditions on the source term E_3 are required for (75). These simple solutions may be used for measuring the material properties in (67) and as the benchmarks of numerical schemes.

6.1. $E_3 = E_3(x_1)$

Since E_3 is independent of x_2, by symmetry we seek a solution of form $w = w(x_1)$ to (74), ie.,

$$\frac{d^2}{dx_1^2}[\kappa_b \frac{d^2}{dx_1^2} w(x_1) + \gamma E_3(x_1)] = 0 \qquad \forall\, x_1 \in \mathbb{R}. \tag{76}$$

The general solution to equation (76) is given by

$$w(x_1) = -\int\int \frac{\gamma}{\kappa_b} E_z(x_1) + C_0 + C_1 x_1, \tag{77}$$

where C_0 and C_1 are the integration constants and shall be determined by boundary conditions. In particular, if the external field is generated by an infinite line charge of line density q along $\mathbf{i}_2$ direction and above the membrane with distance z_0, then

$$E_3(x_1) = -\frac{qz_0}{2\pi\epsilon_0}(z_0^2 + x_1^2)^{-1} \tag{78}$$

Substitute (78) into (77), then we have

$$w(x_1) = \frac{q\gamma}{2\pi\epsilon_0\kappa_b}[x arctan(\frac{x_1}{z_0}) - \frac{z_0}{2} log(x_1^2 + z_0^2)] \tag{79}$$

Fig. 12 shows that the line charge q can cause the deformation of a flexoelectric membrane. In the figure, x is normalized by the distance between the charge and the membrane z_0, $w(x_1)$ is normalized by the term $w_0 = q\gamma/\epsilon_0\kappa_b z_0$. We expect this result to have important implications for the study of lipid bilayers by ions in the surranding electrolytes.

6.2. $E_3 = E_3(r)$

Since E_3 is only a function of $r = (x_1^2 + x_2^2)^{1/2}$, by symmetry we seek a solution $w = w(r)$ to (74)

$$\frac{d}{rdr} r \frac{d}{dr}[\kappa_b \frac{d}{rdr} r \frac{d}{dr} w(r) + \gamma E_3(r)] = 0 \qquad \forall\, r > 0.$$

Neglecting immaterial integration constants, by (75) we have

$$\frac{d}{rdr} r \frac{d}{dr} w(r) = -\frac{\gamma}{\kappa_b} E_3(r) \tag{80}$$

Upon specifying the functional form $E_3(r)$, we can integrate the RHS of (80) explicitly for $w(r)$. In particular, if the external field is generated by a point charge Q above the membrane at $x_3 = z_0$, then

$$E_3(r) = -\frac{qz_0}{4\pi\epsilon_0}(z_0^2 + r^2)^{-3/2} \tag{81}$$

Substitute (81) into (80), then we have

$$w(r) = -\frac{q\gamma}{4\pi\epsilon_0\kappa_b}[log(r) - log(z_0^2 + z_0\sqrt{r^2 + z_0^2})] \tag{82}$$

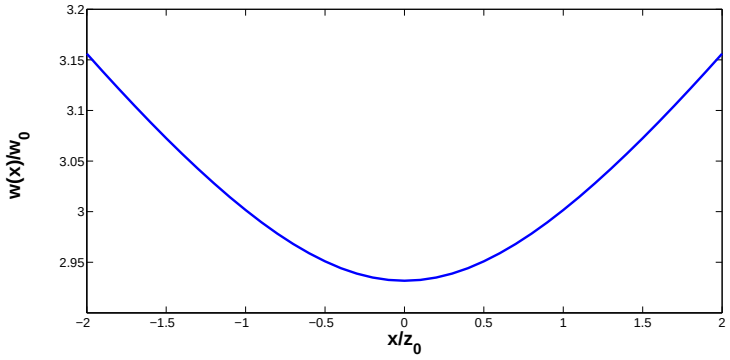

Fig. 12. Deflection of a flexoelectric membrane near a line charge. Reprinted with permission from ELSEVIER.[43] Copyright 2014.

7. Flexoelectricity in Soft Materials

7.1. *1D formulation for soft materials*

In this section, our recent effort to investigate the effect of nonlinearity on flexoelectricity in soft materials[43] is presented. We now consider a one-dimensional system (a thin film) which is composed of soft materials. For this case, the strain of the system is expected to be finite and it is necessary to differentiate between the current and reference configurations. Let (X, Y, Z) be the Lagrangian coordinates of material points, $(\rho_0^e(X), P_0^e(X))$ be the external polarization (along X-direction, per unit volume) and charge density (in the reference configuration), and $b_0^e(X)$, t_0^e be the body force, surface traction (equal and opposite at top and bottom faces) in X-direction, respectively. The electrodes on the top and bottom faces are assumed to be mechanically trivial. Nevertheless, the electrodes are expected to maintain a constant electrostatic potential on both the top and bottom faces.

The electro-elastic state of the film is described by deformation and polarization—these are the independent variables in our formulation. In the presence of external charges, dipoles, applied voltage, and mechanical loads the film is deformed; the deformation is denoted by $(x, y, z) = \boldsymbol{\chi}(X, Y, Z)$ with (x, y, z) being the Eulerian coordinates in the current configuration. Let P be the intrinsic polarization in X-direction per unit volume (in the reference configuration). Since the film is thin (the thickness H is much

smaller than the width L in the other two directions) and transversely isotropic, for simplicity we restrict ourselves to the following class of deformation and polarization:

$$x = X + u(X), \quad y = Y\alpha(X), \quad z = Z\beta(X), \quad P = P(X), \tag{83}$$

where the scalar functions $u, \alpha, \beta, P : (0, H) \to \mathbb{R}$ are determined by the equilibrium conditions. We remark that this kinematic assumption (83) about the possible form of deformation is the equivalent to that in the classic theory of extension. Following the standard framework of nonlinear continuum mechanics, we introduce the *stretches* in X (resp. Y, Z)-direction: $\lambda_1 = 1 + \frac{\partial u}{\partial X}$ (resp. $\lambda_2 = \frac{\partial y}{\partial Y} = \alpha, \lambda_3 = \frac{\partial z}{\partial Z} = \beta$). Thus, the Jacobian becomes $J = \lambda_1\lambda_2\lambda_3 = \det \mathbf{F}$. For brevity, we denote by

$$\boldsymbol{\lambda} = (\lambda_1, \lambda_2, \lambda_3) \qquad \text{and} \qquad \boldsymbol{\Lambda} = (\Lambda_1, \Lambda_2, \Lambda_3) = (\frac{d\lambda_1}{dX}, \frac{d\lambda_2}{dX}, \frac{d\lambda_2}{dX}).$$

Then the governing equations (25) reduce to the following 1D version:

$$\begin{cases} \frac{\partial \psi}{\partial P} - \frac{d}{dX}(\frac{\partial \psi}{\partial \Pi}) + \frac{1}{\lambda_1}\frac{d\phi}{dX} = 0 & \text{on } (0, H), \\ \frac{d}{dX}[\tilde{T}_i + \tilde{\Sigma}_i] + Jb_i^e = 0 & \text{on } (0, H), \\ \frac{d}{dX}[\epsilon_0 \frac{1}{\lambda_1}\phi_{,X} + \frac{P(X)+P_0^e(X)}{J}] = \frac{\lambda_1}{J}\rho_0^e(X) & \text{on } (0, H), \end{cases} \tag{84}$$

where

$$\tilde{T}_i = \frac{\partial \psi}{\partial \lambda_i} - \frac{d}{dX}(\frac{\partial \psi}{\partial \Lambda_i}) \qquad (i = 1, 2, 3), \tag{85}$$

and

$$\begin{aligned} \tilde{\Sigma}_1 &= -\frac{1}{\lambda_1^2}\phi_{,X}(P + P_0^e) + \frac{\epsilon_0 J}{2\lambda_1^3}\phi_{,X}, \\ \tilde{\Sigma}_2 &= -\frac{\epsilon_0 J}{2\lambda_1^2\lambda_2}(\phi_{,X})^2, \qquad \tilde{\Sigma}_3 = -\frac{\epsilon_0 J}{2\lambda_1^2\lambda_2}(3\phi_{,X})^2. \end{aligned} \tag{86}$$

As a special case, we assume that there are no external body force and the surface traction $\mathbf{t}_0^e$ applied in the X direction. Then boundary conditions are given by

$$\begin{cases} \tilde{T}_1 + \tilde{\Sigma}_1 - t_0^e = 0 & \text{at } X = 0 \ \& X = H, \\ \tilde{T}_2 + \tilde{\Sigma}_2 = 0 & \text{at } X = 0 \ \& X = H, \\ \tilde{T}_3 + \tilde{\Sigma}_3 = 0 & \text{at } X = 0 \ \& X = H, \\ \frac{\partial \psi}{\partial \Lambda_1} = \frac{\partial \psi}{\partial \Lambda_2} = \frac{\partial \psi}{\partial \Lambda_3} = 0 & \text{at } X = 0 \ \& X = H, \\ \phi(0) = 0, & \phi(H) = V, \end{cases} \tag{87}$$

where t_0^e is the $X-$ component of $\mathbf{t}_0^e$.

To demonstrate the flexoelectric effects in soft materials, we consider isotropic flexoelectric materials with the internal energy density given by

$$\psi(\boldsymbol{\lambda}, \boldsymbol{\Lambda}, P) = W_{elast}(\boldsymbol{\lambda}) + \frac{g}{2}\Lambda_1^2 + f\Lambda_1 P + \frac{1}{2(\epsilon-\epsilon_0)J}P^2, \tag{88}$$

where $W_{elast}(\boldsymbol{\lambda})$ is the strain energy density function dictating the mechanical properties of materials, the last term implies that the dielectric constant (i.e., permittivity) ϵ of the material is independent of deformation in the absence of flexoelectric effects, i.e., the third term $f\Lambda_1 P$, the second term $\frac{g}{2}\Lambda_1^2$ guarantees that the natural state $(\boldsymbol{\lambda}, \boldsymbol{\Lambda}, P) = (0, 0, 0)$ is the stable equilibrium state of the film in the absence of all external electrical and mechanical loads. Here, constants $f, g > 0, \epsilon > \epsilon_0$ are material properties which can be determined by benchmark experiments.

Inserting (88) into (84), (85),and (87), then we obtain the following governing equations

$$\begin{cases} \frac{P}{(\epsilon-\epsilon_0)J} + f\Lambda_1 + \frac{1}{\lambda_1}\frac{d\phi}{dX} = 0 & \text{on } (0, H), \\ [\frac{\partial W_{elast}}{\partial \lambda_1} + \tilde{\Sigma}_1' - (gu_{,XX} + fP)_{,X}]_{,X} + b_0^e = 0 & \text{on } (0, H), \\ \frac{\partial W_{elast}}{\partial \lambda_2} + \tilde{\Sigma}_2' = 0 & \text{on } (0, H), \\ \frac{\partial W_{elast}}{\partial \lambda_3} + \tilde{\Sigma}_3' = 0 & \text{on } (0, H), \\ \frac{d}{dX}[\epsilon_0 \frac{1}{\lambda_1}\phi_{,X} + \frac{P(X)+P_0^e(X)}{J}] = \frac{\lambda_1}{J}\rho_0^e(X) & \text{on } (0, H), \end{cases} \tag{89}$$

and the boundary conditions

$$\begin{cases} \frac{\partial W_{elast}}{\partial \lambda_1} + \tilde{\Sigma}_1' - (gu_{,XX} + fP)_{,X}] - t_0^e = 0 & \text{at } X = 0 \ \&X = H, \\ gu_{,XX} + fP = 0 & \text{at } X = 0 \ \&X = H, \\ \phi(0) = 0, & \phi(H) = V, \end{cases} \tag{90}$$

where

$$\tilde{\Sigma}_i' = \tilde{\Sigma}_i - \frac{P^2}{2(\epsilon-\epsilon_0)J\lambda_i}$$

We remark that if the elastic properties of the soft materials are specified, e.g. the Neo-Hookean hyperelastic model with (μ, shear modulus; κ, bulk modulus)

$$W_{elast}(\boldsymbol{\lambda}) = \frac{\mu}{2}[J^{-2/3}(\lambda - 1^2 + \lambda_2^2 + \lambda_3^2) - 3] + \frac{\kappa}{2}(J-1)^2, \tag{91}$$

then (89) and (90) form a closed boundary value problem which can be solved to determine the state variables $(\boldsymbol{\chi}, P)$ (i.e., u, α, β, P, and ϕ).

Moreover, if the material is *incompressible* with $J = \lambda_1\lambda_2\lambda_3 = 1$, the state variables as given by (83) shall satisfy

$$J = (1 + u_{,X})\alpha\beta = 1.$$

To incorporate this incompressibility constraint, we use the Lagrange multiplier approach and add to the total free energy:

$$\int_0^H q[(1 + u_{,X})\alpha\beta - 1]dX,$$

where $q : (0, H) \to \mathbb{R}$ can be interpreted as the hydrostatic pressure as in the classic context. Taking into account the hydrostatic term and repeating the similar variational calculations as stated previously, we find the associated Euler-Lagrange equations

$$\begin{cases} \frac{\partial W}{\partial P} + \frac{1}{\lambda_1}\phi_{,X} = 0 & \text{on } (0, H), \\ \frac{d}{dX}[\tilde{T}_1 + \tilde{\Sigma}_1 + \frac{q}{\lambda_1}] + Jb_1^e = 0 & \text{on } (0, H), \\ \tilde{T}_2 + \tilde{\Sigma}_2 + \frac{q}{\lambda_2} = 0 & \text{on } (0, H), \\ \tilde{T}_3 + \tilde{\Sigma}_3 + \frac{q}{\lambda_3} = 0 & \text{on } (0, H), \end{cases} \tag{92}$$

For an incompressible flexoelectric Neo-Hookean material described by (88) and (91), based on symmetry, we note that a solution for the boundary value problem should satisfy

$$\lambda_2 = \alpha = \lambda_3 = \beta = \lambda_1^{-1/2} \qquad \text{on } (0, H). \tag{93}$$

Further, we can rewrite the strain energy density as

$$W_{elast}(\lambda_1) = \frac{\mu}{2}(\lambda_1^2 + \frac{2}{\lambda_1} - 3), \tag{94}$$

which, by(85), $(92)_{3,4}$, and (93), implies

$$\tilde{T}_2 = \tilde{T}_3 = 0, \qquad \tilde{\Sigma}_2 = \tilde{\Sigma}_3 = -q\lambda_1^{1/2} \qquad \text{on } (0, H). \tag{95}$$

Eliminating q in $(92)_{1,2}$ by equatinos (95), we obtain the following explicit boundary value problem for u, ϕ, and P:

$$\begin{cases} \frac{P}{\epsilon - \epsilon_0} + f\lambda_{1,X} + \lambda_1^{-1}\phi_{,X} = 0 & \text{on } (0, H), \\ [\mu(\lambda_1 - \lambda_1^{-2}) + \tilde{\Sigma}_{eq} - (gu_{,XX} + fP)_{,X}]_{,X} + Jb_1^e = 0 & \text{on } (0, H), \\ [-\epsilon_0\lambda_1^{-1}\phi_{,X} + P + P_0^e]_{,X} = \lambda_1\rho_0^e & \text{on } (0, H), \\ \mu(\lambda_1 - \lambda_1^{-2}) + \tilde{\Sigma}_{eq} - (gu_{,XX} + fP)_{,X} - t_0^e = 0 & \text{at } X = 0\&H, \\ gu_{,XX} + fP = 0 & \text{at } X = 0\&H, \\ \phi(0) = 0, & \phi(H) = V, \end{cases} \tag{96}$$

where $\lambda_1 = 1+u_{,X}$, and $\tilde{\Sigma}_{eq} = \tilde{\Sigma}_1 - \lambda_1^{-3/2}\tilde{\Sigma}_2 = -\frac{1}{\lambda_1^2}\phi_{,X}(P+P_0^e) + \frac{\epsilon_0}{\lambda_1^3}(\phi_{,X})^2$.

7.2. *Flexoelectric effects in a soft bilayer structure*

Now we consider the flexoelectric effect in the context of the simple bilayer structure shown in Fig. 13. For this structure, the layer A and B are made of different soft materials. For this problem, the voltage difference between the two surfaces is maintained to be zero throughout the calculation however a uniform loading t_0^e is applied. Under this loading, an electric displacement will ensue in the body. The effective piezoelectricity is then calculated by $d^{eff} = d\tilde{D}/dt_0^e$, where $\tilde{D}$ is the average electric displacement of the bilayer structure.

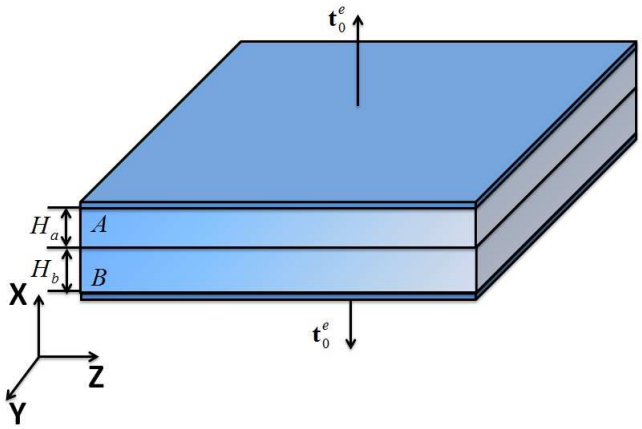

Fig. 13. A bilayer flexoelectric structure under uniform mechanical loading. Reprinted with permission from.[43] Copyright 2014 by ELSEVIER.

In the absence of external polarization, charges and body force, i.e., $P_0^e = b_0^e = \rho_0^e = 0$, by (96) we obtain the following explicit boundary value problem for u, ϕ, and P:

$$\begin{cases} \frac{P}{\epsilon-\epsilon_0} + f\lambda_{1,X} + \lambda_1^{-1}\phi_{,X} = 0 & \text{on } (-H_b, H_a), \\ [\mu(\lambda_1 - \lambda_1^{-2}) + \tilde{\Sigma}_{eq} - (gu_{,XX} + fP)_{,X}]_{,X} + Jb_1^e = 0 & \text{on } (-H_b, H_a), \\ [-\epsilon_0\lambda_1^{-1}\phi_{,X} + P + P_0^e]_{,X} = 0 & \text{on } (-H_b, 0) \cup (0, H_a), \\ \mu(\lambda_1 - \lambda_1^{-2}) + \tilde{\Sigma}_{eq} - (gu_{,XX} + fP)_{,X} - t_0^e = 0 & \text{at } X = -H_b \& H_a, \\ gu_{,XX} + fP = 0, \qquad \phi = 0 & \text{at } X = -H_b \& H_a \end{cases} \tag{97}$$

with the following interfacial conditions

$$\begin{cases} [\![[\mu(\lambda_1 - \lambda_1^{-2}) + \tilde{\Sigma}_{eq} - (gu_{,XX} + fP)_{,X}]_{,X} + Jb_1^e]\!] = 0 \\ [\![[-\epsilon_0 \lambda_1^{-1}\phi_{,X} + P + P_0^e]_{,X}]\!] = 0 \\ [\![gu_{,XX} + fP]\!] = 0, \qquad [\![\phi]\!] = 0 \\ [\![u]\!] = 0, \qquad [\![u_{,X}]\!] = 0 \end{cases} \tag{98}$$

where $[\![\ ]\!] = ()|_{X=0_+} - ()|_{X=0_-}$.

For this problem, we set the displacement on the interface $u(0)$ to be zero to eliminate rigid body motion. Polypropylene cellular film and polyvinylidene fluoride (PVDF) are used for the layer A and B, respectively. The material properties of the two layers are given by

- Layer A: $\mu_a = 0.95MPa$, $\epsilon_a = 2.35\epsilon_0$, $f_a = 46.79Nm/C$, $g_a = 1.28 \times 10^{-8}N$;
- Layer B: $\mu_b = 2.0GPa$, $\epsilon_b = 9.5\epsilon_0$, $f_b = 179Nm/C$, $g_b = 5.42\times10^{-10}N$.

The shear modulus and flexoelectricity coefficient of PVDF are reported in Chu and Salem's work.[42] The shear modulus of polypropylene cellular is from (Qu and Yu,2011).[70] Since there is no report on the flexoelectricity coefficient of polypropylene cellular film, in this work, we have assumed a reasonable value which is within the range of known values for common polymer materials. Also, the value of g has to be estimated. The reader is referred to two works[33,71] that use atomistic and microscopic considerations to determine this parameter that sets the nonlocal elastic length scale. We use a simple route to predict an approximate value for the polymer studied by us. As motivated by Maraganti and Sharma,[33] the characteristic nonlocal elastic length scale can be approximated by the radius of gyration. Accordingly, we set $\sqrt{g/3\mu} \sim R_g$, where R_g is the radius of gyration of the polymer studied.

It is not trivial to analytically solve the boundary value problem described by (97) and (98). In this section, a general purpose finite-element based partial differential equations solver (COMSOL) was used for this purpose. Because of the highly nonlinear natural of the problem, the quartic (4th-order) 1D finite element is used for all the calculations in this section. Another reason for using the higher order element here is that the high order continuity need to be satisfied throughout the specimen.

Fig.14 shows the size effect on the effective piezoelectricity for different stress levels. In this figure, d^{eff} is normalized by d^{BaTiO_3}. Several observations may be made:(i) the effective piezoelectric coefficient shows size

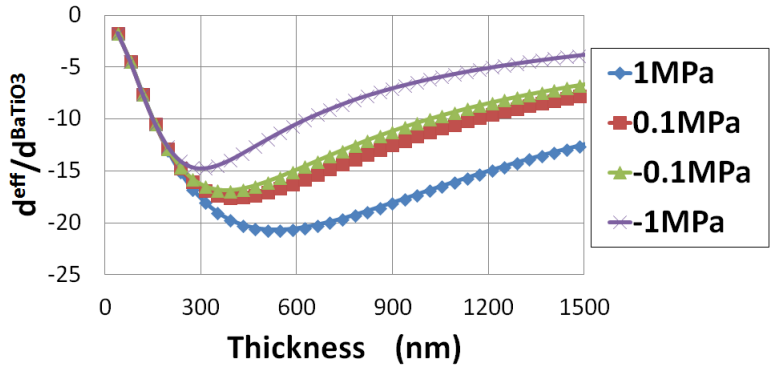

Fig. 14. Flexoelectric effect in a soft bilayer structure. Reprinted with permission from ELSEVIER.[43] Copyright 2014.

effect which can be profitably used to engineer a high electromechanical coupling by exploiting the flexoelectric effect, (ii) the resulting electromechanical coupling in soft material is quite high—reaching to 20 times that of Barium Titanate, and finally, (iii) unlike hard ceramics, the pronounced size-effect is evident even at the micron scale (as opposed to nanoscale). The latter has important ramifications in terms of experimental verification and exploitation for practical applications.

8. Concluding Remarks

In this chapter, we have attempted to provide a comprehensive account of a continuum field theory for flexoelectricity. In particular, we have emphasized a careful development of the nonlinear theory of flexoelectricity which is critical when considering soft materials. We have presented several pedagogical examples that illustrate the important applications of flexoelectricity in the fields of energy harvesting, sensing and actuation, soft active materials, and biological membranes. In particular, we strongly believe that some of the most exciting applications of flexoelectricity will emerge in the area of soft materials.

References

1. L. E. Cross, Flexoelectric effects: Charge separation in insulating solids subjected to elastic strain gradients., *J. Mater. Sci.* **41**, 53–63 (2006).

2. W. Ma and L. E. Cross, Large flexoelectric polarization in ceramic lead magnesium niobate., *Applied Physics Letters.* **79**(19), 4420–4422 (2001).
3. W. Ma and L. E. Cross, Flexoelectric polarization in barium strontium titanate in the paraelectric state., *Applied Physics Letters.* **81**(19), 3440–3442 (2002).
4. W. Ma and L. E. Cross, Strain-gradient induced electric polarization in lead zirconate titanate ceramics., *Applied Physics Letters.* **82**(19), 3923–3925 (2003).
5. W. Ma and L. E. Cross, Flexoelectricity of barium titanate., *Applied Physics Letters.* **88**, 232902 (2006).
6. G. Catalan, L. J. Sinnamon, and J. M. Gregg, The effect of flexoelectricity on the dielectric properties of inhomogeneously strained ferroelectric thin films., *Journal of Physics: Condensed Matter.* **16**(13), 2253–2264 (2004).
7. G. P. Zubko, A. R. Catalan, P. Buckley, L. Welche, and J. F. Scott, Strain-gradient induced polarization in srtio_3 single crystals., *Physical Review Letters.* **99**, 167601 (2007).
8. J. Y. Fu, W. Zhu, N. Li, and L. E. Cross, Experimental studies of the converse flexoelectric effect induced by inhomogeneous electric field in a barium strontium titanate composition., *Journal of Applied Physics.* **100**, 024112 (2006).
9. J. Y. Fu, W. Zhu, N. Li, and L. E. Cross, Gradient scaling phenomenon in microsize flexoelectric piezoelectric composites., *Applied Physics Letters.* **91**, 182910 (2007).
10. E. A. Eliseev, A. N. Morozovska, M. D. Glinchuk, and R. Blinc, Spontaneous flexoelectric/flexomagnetic effect in nanoferroics., *Physical Review B.* **79**, 165433 (2009).
11. E. A. Eliseev, M. D. Glinchuk, V. Khist, V. V. Skorokhod, R. Blinc, and A. N. Morozovska, Linear magnetoelectric coupling and ferroelectricity induced by the flexomagnetic effect in ferroics., *Physical Review B.* **84**, 174112 (2011).
12. R. Maranganti and P. Sharma, Atomistic determination of flexoelectric properties of crystalline dielectrics., *Physical Review B.* **80**, 054109 (2009).
13. M. S. Majdoub, P. Sharma, and T. Cagin, Enhanced size-dependent piezoelectricity and elasticity in nanostructures due to the flexoelectric effect., *Physical Review B.* **77**, 125424 (2008).
14. M. S. Majdoub, P. Sharma, and T. Cagin, Dramatic enhancement in energy harvesting for a narrow range of dimensions in piezoelectric nanostructures., *Physical Review B.* **78**, 121407(R) (2008).
15. M. S. Majdoub, P. Sharma, and T. Cagin, Erratum: Enhanced size-dependent piezoelectricity and elasticity in nanostructures due to the flexoelectric effect., *Physical Review B.* **79**, 119904(E) (2009).
16. M. S. Majdoub, P. Sharma, and T. Cagin, Erratum: Dramatic enhancement in energy harvesting for a narrow range of dimensions in piezoelectric nanostructures., *Physical Review B.* **79**, 159901(E) (2009).
17. N. D. Sharma, R. Maranganti, and P. Sharma, On the possibility of piezoelectric nanocomposites without using piezoelectric materials., *Journal of the Mechanics and Physics of Solids.* **55**, 2328–2350 (2007).

18. N. D. Sharma, C. M. Landis, and P. Sharma, Piezoelectric thin-film superlattices without using piezoelectric materials., *Journal of Applied Physics.* **108**, 024304 (2010).
19. N. D. Sharma, C. M. Landis, and P. Sharma, Erratum: Piezoelectric thin-film superlattices without using piezoelectric materials., *Journal of Applied Physics.* **111**, 059901 (2012).
20. M. Gharbi, Z. H. Sun, P. Sharma, K. White, and S. El-Borgi, Flexoelectric properties of ferroelectrics and the nanoindentation size-effect., *International Journal of Solids and Structures.* **48**, 249–256 (2011).
21. S. V. Kalinin and V. Meunier, Electronic flexoelectricity in low-dimensional systems., *Physical Review B.* **77**(3), 033403 (2008).
22. T. Dumitrica, C. M. Landis, and B. I. Yakobson, Curvature induced polarization in carbon nanoshells., *Chemical Physics Letters.* **360**(1–2), 182–188 (2002).
23. A. K. Tagantsev, Theory of flexoelectric effect in crystals., *Sov. Phys. JETP.* **61**(6), 1246–1254 (1985).
24. A. K. Tagantsev, Piezoelectricity and flexoelectricity in crystalline dielectrics., *Physical Review B.* **34**, 5883–5889 (1986).
25. A. K. Tagantsev, Electric polarization in crystals and its response to thermal and elastic perturbations., *Phase Transit.* **35**(3-4), 119–203 (1986).
26. A. K. Tagantsev, V. Meunier, and P. Sharma, Novel electromechanical phenomena at the nanoscale: phenomenological theory and atomistic modeling., *MRS Bulletin.* **34**(9), 643–647 (2009).
27. R. Maranganti, N. D. Sharma, and P. Sharma, Electromechanical coupling in nonpiezoelectric materials due to nanoscale nonlocal size effects: Green's function solutions and embedded inclusions., *Physical Review B.* **74**, 014110 (2006).
28. T. D. Nguyen, S. Mao, Y. W. Yeh, P. K. Purohit, and M. C. McAlpine, Nanoscale flexoelectricity., *Adv Mater.* **25**(7), 946–974 (2013).
29. S. Chandratre and P. Sharma, Coaxing graphene to be piezolectric., *Applied Physics Letters.* **100**, 023114 (2012).
30. A. G. Petrov, *Flexoelectric model for active transport. In: Physical and chemical bases of biological information transfer.* Plenum Press, New York (1975).
31. A. G. Petrov, Flexoelectricity of model and living membranes., *Biochim. Biophys. Acta.* **1561**, 1–25 (2002).
32. A. G. Petrov, Flexoelectricity and mechanotransduction., *Current Topics in Membranes: Mechanosensitive Ion Channels, Part A.* **58**, 121–150 (2007).
33. R. Maranganti and P. Sharma, A novel atomistic approach to determine strain-gradient elasticity constants: Tabulation and comparison for various metals, semiconductors, silica, polymers and the (ir) relevance for nanotechnologies., *Journal of the Mechanics and Physics of Solids.* **55**(9), 1823–1852 (2007).
34. T. Xu, J. Wang, T. Shimada, and T. Kitamura, Direct approach for flexoelectricity from first-principles calculations: cases for srtio3 and batio3., *Journal of Physics: Condensed Matter.* **25**(41), 415901 (2007).
35. J. Hong, G. Catalan, J. F. Scott, and E. Artacho, The flexoelectricity of bar-

ium and strontium titanatesfrom first principles., *Journal of Physics: Condensed Matter.* **22**(11), 112201 (2010).
36. J. Hong and D. Vanderbilt, First-principles theory of frozen-ion flexoelectricity., *Physical Review B.* **84**, 180101 (2011).
37. J. Hong and D. Vanderbilt, First-principles theory and calculation of flexoelectricity., *Physical Review B.* **88**, 174107 (2013).
38. M. Stengel, Flexoelectricity from density-functional perturbation theory., *Physical Review B.* **88**, 174106 (2013).
39. M. Stengel, Microscopic response to inhomogeneous deformations in curvilinear coordinates., *Nature Communications.* **4**, 2693 (2013).
40. S. Baskaran, X. He, Q. Chen, and J. Y. Fu, Experimental studies on the direct flexoelectric effect in α-phase polyvinylidene fluoride films., *Applied Physics Letters.* **98**, 242901 (2011).
41. S. Baskaran, X. He, Y. Wang, and J. J. Y. Fu, Strain gradient induced electric polarization in α-phase polyvinylidene fluoride films under bending conditions., *Journal of Applied Physics.* **111**, 014109 (2012).
42. B. Chu and D. R.Salem, Flexoelectricity in several thermoplastic and thermosetting polymers., *Applied Physics Letters.* **101**, 103905 (2012).
43. Q. Deng, L. Liu, and P. Sharma, Flexoelectricity and electrets in soft materials and biological membranes., *Journal of the Mechanics and Physics of Solids.* **62**, 209–227 (2014).
44. G. Catalan, A. Lubk, A. Vlooswijk, E. Snoeck, C. Magen, A. Janssens, G. Rispens, G. Rijnders, D. Blank, and B. Noheda, Flexoelectric rotation of polarization in ferroelectric thin films, *Nature Materials.* **10**(12), 963–967 (2011).
45. M. S. Majdoub, R. Maranganti, and P. Sharma, Understanding the origins of the intrinsic dead layer effect in nanocapacitors., *Physical Review B.* **79**, 115412 (2009).
46. P. Zubko, G. Catalan, and A. K. Tagantsev, Flexoelectric effect in solids., *Annu. Rev. Mater. Res.* **43**, 387–421 (2013).
47. P. V. Yudin and A. K. Tagantsev, Fundamentals of flexoelectricity in solids., *Nanotechlology.* **24**, 432001 (2013).
48. S. Shen and S. Hu, A theory of flexoelectricity with surface effect for elastic dielectrics., *Journal of the Mechanics and Physics of Solids.* **58**, 665–677 (2010).
49. S. Dai, M. Gharbi, P. Sharma, and H. Park, Surface piezoelectricity: size effects in nanostructures and the emergence of piezoelectricity in non-piezoelectric materials., *Journal of Applied Physics.* **110**, 104305 (2011).
50. R. Resta and D. Vanderbilt, Theory of polarization:a modern approach, *Physics of Ferroelectrics: Topics and Applied Physics.* **105**, 31–68 (2007).
51. J. Marshall and K. Dayal, Atomistic-to-continuum multiscale modeling with long-range electrostatic interactions in ionic solids, *Journal of the Mechanics and Physics of Solids.* **62**, 137–162 (2014).
52. R. A. Toupin, The elastic dielectric., *J. Rational Mech. Anal.* **5**(6), 849–915 (1956).
53. R. Bustamante, A. Dorfmann, and R. W. Ogden, Nonlinear electroelasto-

statics: a variational framework., *Z. angew. Math. Phys.* **60**, 154–177 (2009).
54. L. Liu, An energy formulation of continuum magneto-electro-elasticity with applications., *Journal of the Mechanics and Physics of Solids.* **63**, 451–480 (2014).
55. A. S. Yurkov, Elastic boundary conditions in the presence of the flexoelectric effect., *JETP Letters.* **94**(6), 455–458 (2011).
56. R. D. Mindlin, Polarization gradient in elastic dielectrics., *International Journal of Solids and Structures.* **4**, 637–642 (1968).
57. S. Mao and P. Purohit, Insights into flexoelectric solids from strain-gradient elasticity, *Journal of Applied Mechanics.* **81**(8), 081004 (2014).
58. A. Abdollahi, D. Millan, C. Peco, M. Arroyo, and I. Arias, Revisiting pyramid compression to quantify flexoelectricity: A three-dimensional simulation study, *Physical Review B.* **91**, 104103 (2015).
59. Q. Deng, M. Kammoun, A. Erturk, and P. Sharma, Nanoscale flexoelectric energy harvesting., *International Journal of Solids and Structures.* **51**(18), 3218–3225 (2014).
60. A. Erturk and D. J. Inman, *Piezoelectric Energy Harvesting.* Wiley, New Delhi (2011).
61. A. Erturk, Assumed-modes modeling of piezoelectric energy harvesters: Euler-bernoulli, rayleigh, and timoshenko models with axial deformations., *Comput. Struct.* **106–107**, 3218–3225 (2012).
62. R. M. Clough and J. Penzien, *Dynamics of structures. 2nd ed.* McGraw Hill, New York (1993).
63. A. G. Petrov, B. A. Miller, K. Hristova, and P. N. R. Usherwood, Flexoelectric effects in model and native membranes containing ion channels., *European Biophysics Journal.* **22**, 289–300 (1993).
64. W. E. Brownell, A. A. Spector, R. M. Rapheal, and A. S. Popel, Micro- and nanomechanics of the cochlear outer hair cell., *Annu. Rev. Biomed. Eng.* **3**, 169–194 (2001).
65. W. E. Brownell, B. Farrell, and R. M. Rapheal, Membrane electromechanics at hair-cell synapses., *Biophysics of the Cochlea: From Molecules to Models.* pp. 169–176 (2003).
66. R. M. Rapheal, A. S. Popel, and W. E. Brownell, A membrane bending model of outer hair cell electromotility., *Biophysics Journal.* **78**(6), 2844–2862 (2000).
67. K. D. Breneman and R. D. Rabbitt, Piezo- and flexoelectric membrane underlie fast biological motors in the ear., *Materials Research Society Symposium Proceedings.* p. 1186E (2009).
68. P. Mohammadi, L. Liu, and P. Sharma, A theory of flexoelectric membranes and effective properties of heterogeneous membranes., *Journal of Applied Mechanics.* **81**(1), 011007 (2014).
69. W. Helfrich, Elastic properties of lipid bilayers: theory and possible experiments., *Z. Naturforsch C.* **28**(11), 693–703 (1973).
70. S. Qu and Y. Yu, Electromechanical coupling properties and stability analysis of ferroelectrets., *J. Appl. Phys.* **110**, 043525 (2011).
71. S. Nikolov, C. S. Han, and D. Raabe, On the origin of size effects in small-

strain elasticity of solid polymers., *International Journal of Solids and Structures*. **44**(5), 1582–1592 (2007).